Cortical Structure, DWI and Tractography Report concerning S10313 (Initials: JT)

Innovision-IP

August 16, 2024

Contents

1 Summary of findings **3**
- 1.1 Participant Information . . . 3

2 Summary **3**
- 2.1 Main Findings . . . 3
- 2.2 Background to this report . . . 4
- 2.3 Procedural Summary . . . 5

3 Brain Tract Metrics **7**

4 Tracts with changes in the DWI metrics **7**
- 4.1 **Thalamic Radiation Anterior Right Anatomy** . . . 8
- 4.2 **Thalamic Radiation Anterior Right Metrics** . . . 9
- 4.3 **Parietopontine Tract Right Anatomy** . . . 10
- 4.4 **Parietopontine Tract Right Metrics** . . . 11
- 4.5 **Superior Longitudinal Fasciculus 3 Right Anatomy** . . . 12
- 4.6 **Superior Longitudinal Fasciculus 3 Right Metrics** . . . 13
- 4.7 **Superior Longitudinal Fasciculus 2 Left Anatomy** . . . 14
- 4.8 **Superior Longitudinal Fasciculus 2 Left Metrics** . . . 15
- 4.9 **Middle Longitudinal Fasciculus Right Anatomy** . . . 16
- 4.10 **Middle Longitudinal Fasciculus Right Metrics** . . . 17
- 4.11 **Corticospinal Tract Right Anatomy** . . . 18
- 4.12 **Corticospinal Tract Right Metrics** . . . 19
- 4.13 **Dentatorubrothalamic Tract Right Anatomy** . . . 20
- 4.14 **Dentatorubrothalamic Tract Right Metrics** . . . 21
- 4.15 **Frontal Aslant Tract Right Anatomy** . . . 22
- 4.16 **Frontal Aslant Tract Right Metrics** . . . 23
- 4.17 **Corticostriatal Pathway Superior Left Anatomy** . . . 24
- 4.18 **Corticostriatal Pathway Superior Left Metrics** . . . 25
- 4.19 **Superior Longitudinal Fasciculus 2 Right Anatomy** . . . 26

4.20 **Superior Longitudinal Fasciculus 2 Right Metrics** 27

5 Cortical thickness findings **28**
5.1 Left side decreases in cortical thickness 28
5.2 Left side decreases in cortical thickness overlaid onto YEO functional networks 29

6 Cortical myelin findings **30**
6.1 Left side decreases in cortical myelin 31
6.2 Right side decreases in cortical myelin 34
6.3 Left side decreases in cortical myelin overlaid onto YEO functional networks 37
6.4 Right side decreases in cortical myelin overlaid onto YEO functional networks 40
6.5 Left side increases in cortical myelin 43
6.6 Right side increases in cortical myelin 46
6.7 Left side increases in cortical myelin overlaid onto YEO functional networks 49
6.8 Right side increases in cortical myelin overlaid onto YEO functional networks 52

7 Biographies of the authors of this document **55**
7.1 Professor G. Green 55

1 Summary of findings

This report describes the findings of the investigation of white matter tracts, cortical thickness and cortical myelin in the referred individual, **JT**, date of birth 27 Dec 1982, of Bank Cottage, Main Road, Bredon, Tewkesbury, England, GL20 7EL .

1.1 Participant Information

JT	date of birth	27 Dec 1982
JT	client reference number	S10313

Event	by	date
Referred	Rylands	01 Aug 2024
MRI Scan	Cardiff Neuroimaging Facility	13 Aug 2024
Data Received	Innovision-IP	14 Aug 2024
Data Analysed	Innovision-IP	14 Aug 2024

2 Summary

2.1 Main Findings

One of the predictions of bio-engineering analyses of the effects of high de-acceleration or acceleration of the brain within the skull is that white matter tracts are particularly prone to the effects of strain forces in the deep tracts as well as the axons of the tracts as they enter or leave the cortex of the brain [14]. Therefore, Diffusion Weighted Imaging was used to investigate the integrity of the white matter within the brain. The main findings of the analysis of the brain tracts of participant **JT** are that many tracts show highly significant differences when compared to age and gender-matched controls. The ten most affected tracts are described in this report.

Both bioengineering modelling as well as previous observations from DWI analyses have shown that different metrics can be used to characterise the diffusion within each of the brain tracts that were estimated from the MRI DWI scan data. These are fractional anisotropy, radial diffusivity, axial diffusivity, and mean diffusivity. These theoretical modelling predictions which have been confirmed by histological examination of white matter tracts, show that these metrics reflect different aspects of the pathology of brain injury. Here the metrics are measured along each tract and a profile of the measures are statistically compared between the data from **JT** and a set of age and gender-matched controls.

Damage to a white matter tract could lead to both anterograde and retrograde degeneration of the axons of the tract, which in turn could lead to neuronal loss and a loss of myelin within the cortex. Direct local damage to the cortex could also lead to neuronal loss. Neuronal loss is reflected in a decrease in the thickness of the cortex. This has been reported in many publications of the effects of brain injury on the brain. Cortical myelin levels are normally extraordinarily stable during life. Decreases in myelin content, demyelination, has been observed following a head injury. It is also a feature of many demyelinating diseases, such as Multiple Sclerosis. Many neurodegenerative diseases and psychiatric problems such as depression are associated with large decreases in cortical myelination. Increases in myelination are associated with experience dependent changes in cortical microarchitecture, including learning, but have also been observed following regenerative processes within the cortex in animal studies. This is known to be due to to the regeneration of oligodendrocytes following brain damage.

Structural T1 and T2 weighted MRI scans were analysed to investigate if statistically significant differences, from data from a set of control individuals, of cortical thickness and cortical myelin were observed in the brain of **JT**.

2.2 Background to this report

The purpose of the report is to describe whether the white matter tracts, the cortical thickness and the cortical myelin **JT** are within the normal range and, if not, the report shows where in the brain these measures are not within the normal range. T1, T2 weighted Images and Diffusion Weighted Images were collected by using a Magnetic Resonance Imaging (MRI) scanner. This device is used to non-invasively record the structure of the brain and the ease with which water can diffuse in any given direction in the human brain and from this information, various metrics of the cortex and white matter tracts of the brain were estimated.
Analyses of the T1 and T2 weighted images were used to estimate cortical thickness and cortical myelin. For these cortical measures, statistical analysis contained data from 128 individuals.
Analyses of images related to water diffusion using Diffusion Weighted Imaging (DWI) in a MRI scanner typically consider how water can microscopically diffuse in any given direction in the tissue from which the measurement is made. Thus the typically reported term of "diffusivity" (rather than diffusion can be interpreted in such a way that higher values mean that it is easier for water to move in a measured direction, and values approaching zero mean that diffusion in the measured direction alone is far less likely. Changes in diffusivity are known to occur after a head injury and also that the different metrics of DWI analysis correlate with the histological findings after injury [19].The estimates of water diffusivity were compared with data from an age and gender matched control group of individuals from a control population who have no known history of having had a brain injury. The age was matched to be within 10 years. The matched control group for diffusion statistical analysis contained data from 65 individuals. Statistical comparisons were made to compare the referred individual's brain pathways with the controls' data. The analysis investigates the differences in up to 77 regional white matter tracts. These tracts were selected because they have recently been extensively characterised in a large international study of over 1900 "neuro-normal" subjects [3, 5]. This report describes the most significant statistical differences that have been found.
The report was compiled on August 16, 2024 by Gary Green MA DPhil BM BCh and Andre Gouws BSc PhD of Innovision-IP Ltd concerning participant **JT**.

Innovision IP Ltd
+44(0)1865 306286

Culham Innovation Centre
D5 Culham Science Centre
Abingdon, OX14 3DB

2.3 Procedural Summary

Participant **JT** was placed supine in a Magnetic Resonance Imaging (MRI) scanner. There was no task required of the participant. Structural T1 weighted and T2 weighted MRI scans were undertaken of their head. This allowed the anatomy of the brain to be co-registered to the set of control brains to allow for statistical comparisons of the brain tracts, cortical thickness and myelin as well as to allow visualisation of the results. The brain tracts were estimated by acquiring and analysing Diffusion Weighted Images (DWI) [2] of the brain of both **JT** and the controls.
The T1 and T2 weighted images were used to estimate the thickness of the cortex and the cortical myelin content at 32492 locations. The estimates of cortical thickness and myelin were compared with data from an age and gender matched control group of individuals from a control population who have no known history of having had a brain injury. The age was matched to be within 10 years. The matched control group contained data from 128 individuals. Statistical comparisons were made to compare the referred individual's brain with the controls' data. Permutation and cluster methods were used to manage the Family-Wise Error rate or Type I errors. The report describes the differences in 360 regional anatomical parcellations of the cortex as well as 7 functional networks between cortical areas.
DWI data is acquired using MRI protocols that are sensitive to the microscopic diffusion of water molecules. This is achieved by adding magnetic field gradients to the MRI pulse sequences. The field gradients are added such that any diffusion parallel to the gradient directions will decrease the signal recorded in the MRI scanner by interfering with the dephasing and rephasing of the nuclear spins of Hydrogen atoms in the water. The number of orientations of the gradients, the so called b-vectors and the b-values, which is a measure of the gradient strength, how long the magnetic gradient is applied and how long the diffusion is allowed to proceed, all determine the sensitivity and resolution of the resultant image [22].
The DWI data was analysed to correct for eddy current and phase distortions introduced by the imaging process. The brain is divided into voxels each of 2mm resolution and then a model-based approach was used to estimate the water diffusion within each voxel of the brain. This allows the reconstruction of the fibre orientations in each voxel of the brain. This is described as the diffusion tensor and can be used to estimate various metrics at each location as well as to reconstruct the fibre pathways within the brain. This is termed Diffusion Tractography Imaging (DTI) [17]. For this report four metrics are estimated [16, 9]. These are:

- Fractional Anisotropy (FA): This is a measure of the degree of anisotropy in the diffusion of water. If the diffusion is only in one direction, then this measure approaches unity, whereas if the diffusion is freely in all directions, then this measure approaches zero.
- Mean Diffusivity (MD): This is the average of the degree to which diffusion is in the 3 principal directions within the axonal fibres. This is the average of the first, second and third components of the diffusion tensor.
- Axial Diffusivity (AD): This is a measure of the degree to which diffusion is in the direction along the axonal fibres. This is the first component of the diffusion tensor.
- Radial Diffusivity (RD): This is a measure of the degree to which diffusion is in the direction across the axonal fibres. This is the average of the second and third components of the diffusion tensor.

The measures are estimated along the length of each of the reconstructed brain tracts. Data from each location are used to make a statistical comparison with the same measures in the brain tracts of the control individuals. For the statistical comparison of the diffusion metrics with a matched control group

data from 65 individuals were used. It should be noted that as the ends of a tract vary from individual to individual, often due to different cortical folding patterns, only the core of each tract is analysed. For each tract, the anatomical location of the tract, the cortical regions that is connected to and the functional network that it belongs to are shown along with the statistical changes within the tract.
A statistical method of comparing the mean metric in a single subject with the mean metric in a set of control individuals was used. This generates a Studentś T test value at each location which is the difference in the means scaled by the standard error of the variation within the controls. But if one were to perform this statistical test at individual locations along each fibre tract then one would have a multiple comparison problem where statistical differences that arise from chance could give rise to Type 1 statistical errors. To control for this, the statistical method used permutation tests coupled to detecting clusters of statistically significant results along the pathway. This allows the test of the null hypothesis that the data from the single test subject comes from the same probability distribution of the controls. However, caution is required in the interpretation of the cluster as the rejection of the null hypothesis is simply that the single test subject does not belong to the control group and not that there is a significant cluster at a specific position along the tract. One should interpret the results as that a significant change exists within a specific pathway [15].
A commonly used way of presenting the Diffusion characteristic within each tract is to use the mean of the metric along the tract as a single measure and compare that to the mean and variance of the that metric for each of the controls. Each figure below also shows this way of comparing the single client with the controls. For each tract, the mean and variance of the control data for the whole tract is plotted to the right of information within the tract. The controls data and 99.9% confidence limits are in black and the referred individual mean is shown in red.

3 Brain Tract Metrics

- The white matter of the brain, the axonal fibres connecting brain regions, was analysed in terms of the diffusivity of water within these tracts.
- The diffusivity is estimated along a fibre pathway and across the fibre. This is described as four metrics, the fractional anisotropy, the mean diffusivity, the axial diffusivity and the radial diffusivity at 100 locations along each brain tract
- A statistical comparison was made for each brain tract between those of subject and the same tracts in the controls. This was achieved using a permutation-cluster T test of the differences in means of the four metrics along the brain tracts.

The main findings are displayed graphically below, showing the mean difference between control data and that observed in **JT**. Only the 10 most significantly affected tracts are shown in this report. For each tract the location of the tract is shown overlaid on the brain.

4 Tracts with changes in the DWI metrics

A number of studies have demonstrated that changes in the diffusivity measured used here correlate with histological findings in head injury [4, 1, 20, 20, 21, 18]. In humans, DWI has been shown to be useful in the detection of structural abnormalities in TBI in both the acute and chronic phase [12]; the identification of oedema after injury [8]; in predicting neuropsychological correlates of injury [7] amongst many other findings [22, 11].
It should be noted that some DWI studies have shown that DWI changes are only seen in the acute phase after injury [13] ; that fractional anisotropy metrics may be too subtle in mild head injury [10]; and that the use of a single diffusion metric may be difficult to interpret [6]
In the figures below, for each brain tract, there is a picture of the location of the tract within the brain, and four graphs showing the metrics estimated along each tract. These are for the fractional anisotropy, the mean diffusivity, axial diffusivity and radial diffusivity. In each figure the mean for the control group results is shown as a dotted black line, the mean for **JT** is shown as a solid red line. The 99.99% confidence limits for the control group are shown in grey around the control mean. Locations are highlighted where the mean of the control group are higher than that of the single test subject are shown in pink, and where the test subject mean is higher than the control group mean is shown in a yellow colour. Again it should be noted that the interpretation of these clusters is simply that the null hypothesis that the test subject data is within that of the control population, can be rejected.

4.1 Thalamic Radiation Anterior Right Anatomy

This page shows the relationship between the white matter tract, the cortical areas it is connected to and the functional network that the cortical regions belong to.

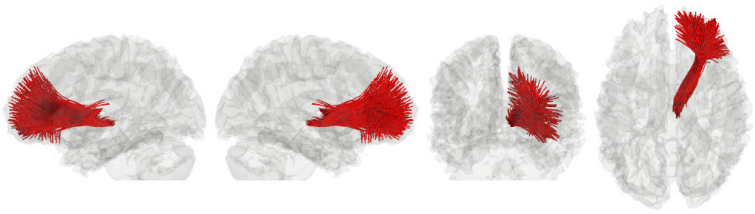

Figure 1: The location of the tract within the brain

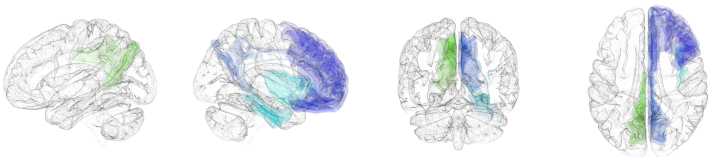

Figure 2: The anatomical areas connected to this tract.

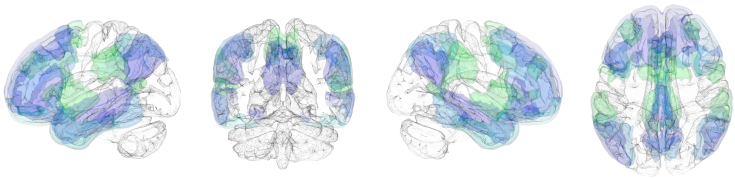

Figure 3: The cortical areas that belong to the functional networks connected to this tract.

4.2 Thalamic Radiation Anterior Right Metrics

The DWI metrics as a function of distance along the tract. Significant increases above the control mean for the test subject are shown shaded in yellow and significant decreases are shown in red. To the right of each subplot is the mean and confidence limit of the control data for the whole tract (black) and the mean of the whole tract for the referred individual (red)
Please note that the direction of what is meant by axial and radial is a function of the orientation of the tract within the brain and may vary along the tract. It should also be noted that some tracts end in the spinal cord and this is not shown in these figures.

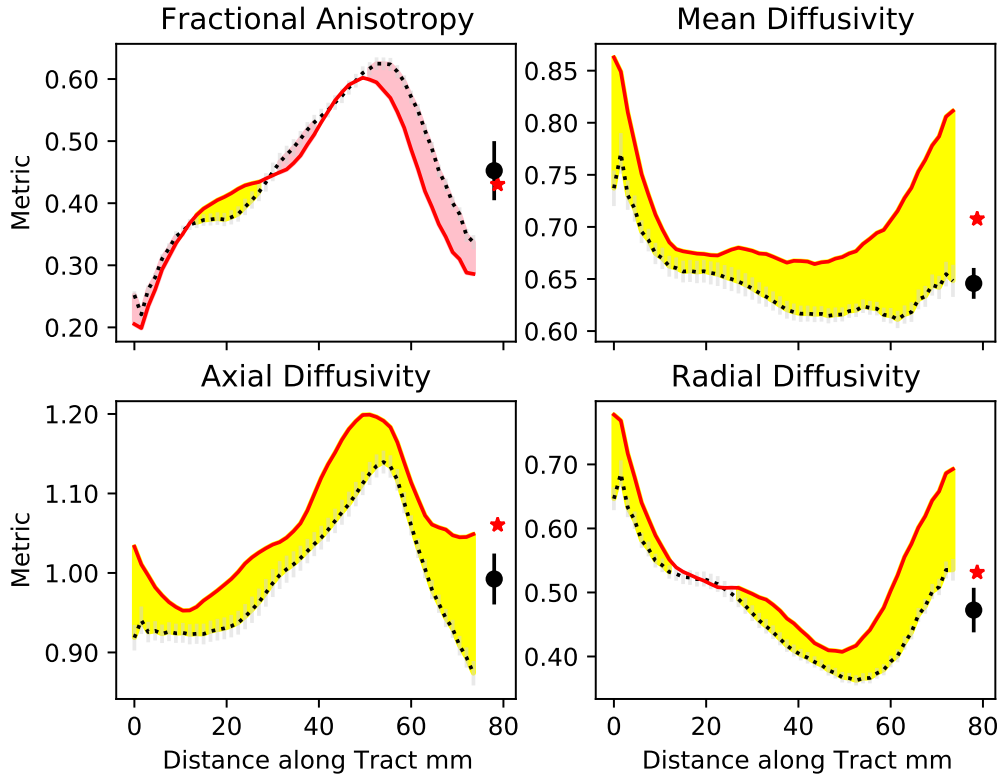

4.3 Parietopontine Tract Right Anatomy

This page shows the relationship between the white matter tract, the cortical areas it is connected to and the functional network that the cortical regions belong to.

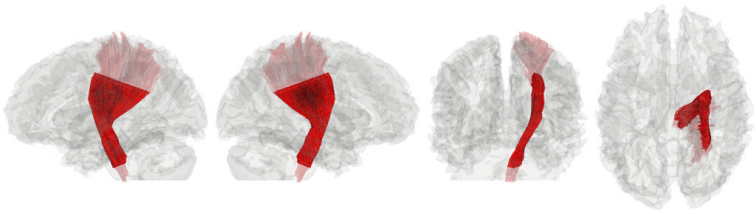

Figure 4: The location of the tract within the brain

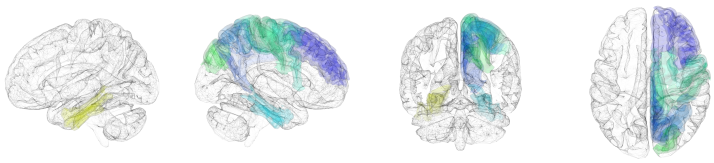

Figure 5: The anatomical areas connected to this tract.

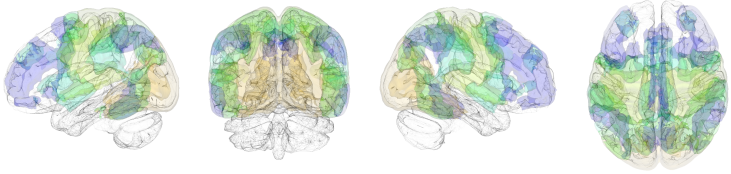

Figure 6: The cortical areas that belong to the functional networks connected to this tract.

4.4 Parietopontine Tract Right Metrics

The DWI metrics as a function of distance along the tract. Significant increases above the control mean for the test subject are shown shaded in yellow and significant decreases are shown in red. To the right of each subplot is the mean and confidence limit of the control data for the whole tract (black) and the mean of the whole tract for the referred individual (red)
Please note that the direction of what is meant by axial and radial is a function of the orientation of the tract within the brain and may vary along the tract. It should also be noted that some tracts end in the spinal cord and this is not shown in these figures.

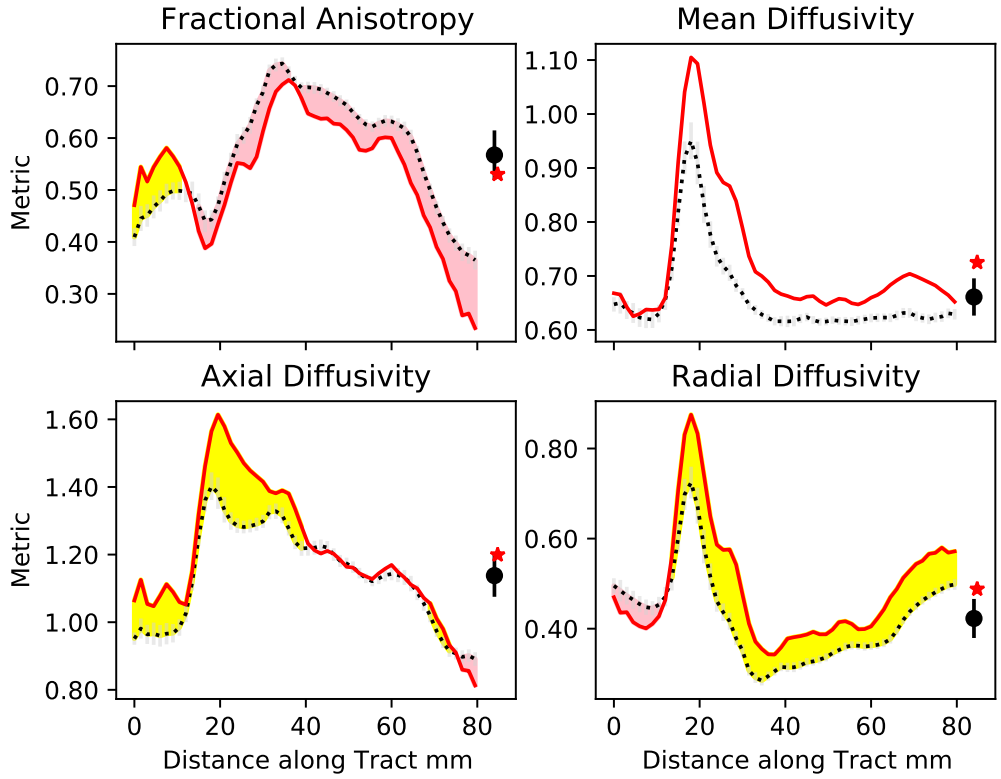

4.5 Superior Longitudinal Fasciculus 3 Right Anatomy

This page shows the relationship between the white matter tract, the cortical areas it is connected to and the functional network that the cortical regions belong to.

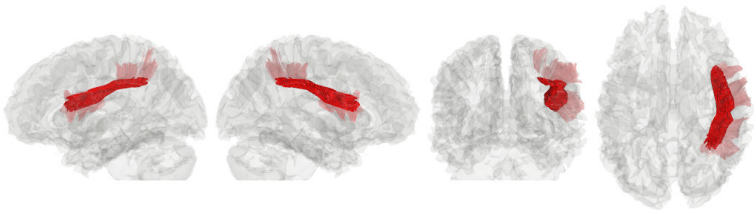

Figure 7: The location of the tract within the brain

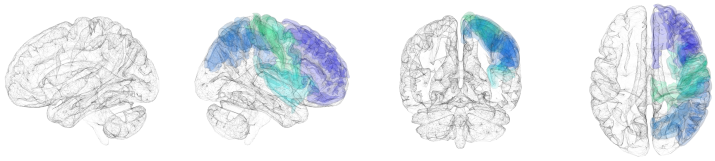

Figure 8: The anatomical areas connected to this tract.

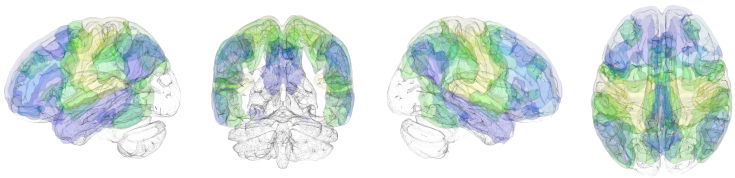

Figure 9: The cortical areas that belong to the functional networks connected to this tract.

4.6 Superior Longitudinal Fasciculus 3 Right Metrics

The DWI metrics as a function of distance along the tract. Significant increases above the control mean for the test subject are shown shaded in yellow and significant decreases are shown in red. To the right of each subplot is the mean and confidence limit of the control data for the whole tract (black) and the mean of the whole tract for the referred individual (red)
Please note that the direction of what is meant by axial and radial is a function of the orientation of the tract within the brain and may vary along the tract. It should also be noted that some tracts end in the spinal cord and this is not shown in these figures.

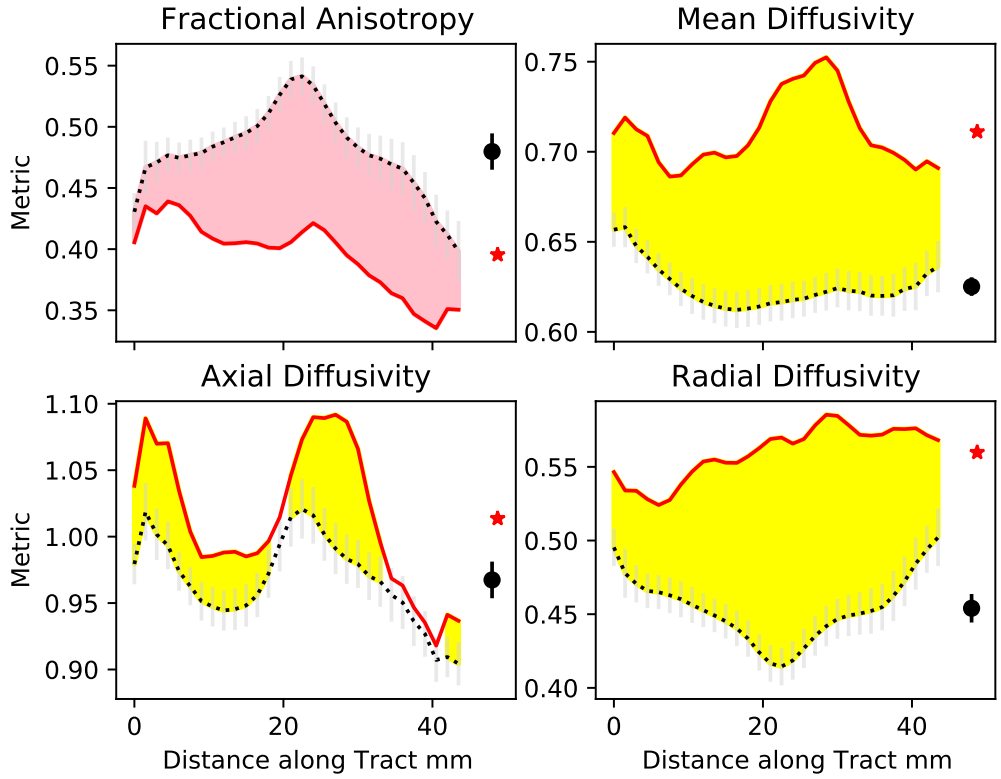

4.7 Superior Longitudinal Fasciculus 2 Left Anatomy

This page shows the relationship between the white matter tract, the cortical areas it is connected to and the functional network that the cortical regions belong to.

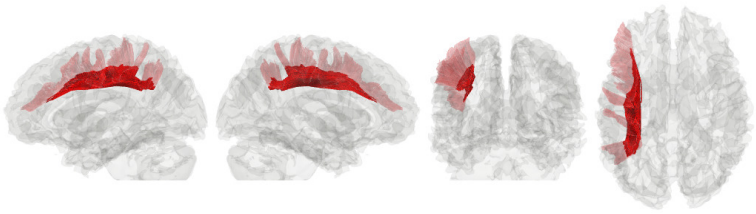

Figure 10: The location of the tract within the brain

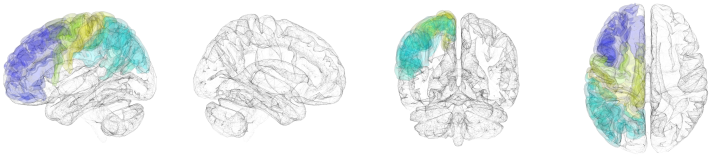

Figure 11: The anatomical areas connected to this tract.

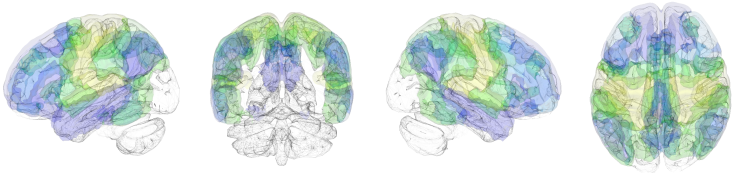

Figure 12: The cortical areas that belong to the functional networks connected to this tract.

4.8 Superior Longitudinal Fasciculus 2 Left Metrics

The DWI metrics as a function of distance along the tract. Significant increases above the control mean for the test subject are shown shaded in yellow and significant decreases are shown in red. To the right of each subplot is the mean and confidence limit of the control data for the whole tract (black) and the mean of the whole tract for the referred individual (red)
Please note that the direction of what is meant by axial and radial is a function of the orientation of the tract within the brain and may vary along the tract. It should also be noted that some tracts end in the spinal cord and this is not shown in these figures.

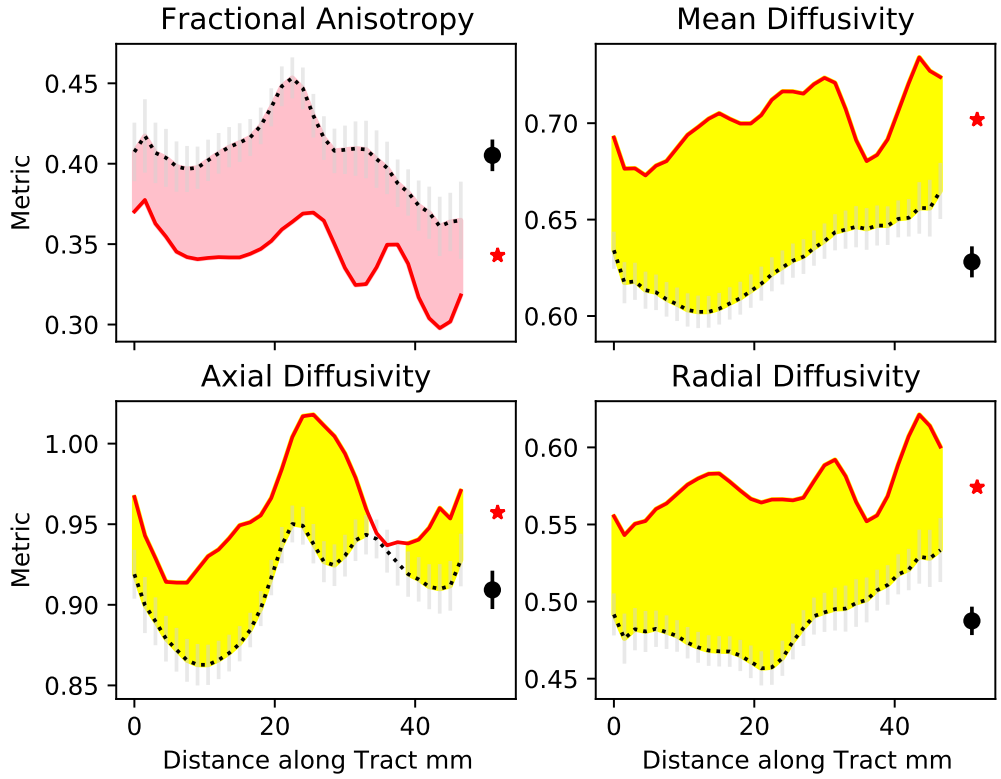

4.9 Middle Longitudinal Fasciculus Right Anatomy

This page shows the relationship between the white matter tract, the cortical areas it is connected to and the functional network that the cortical regions belong to.

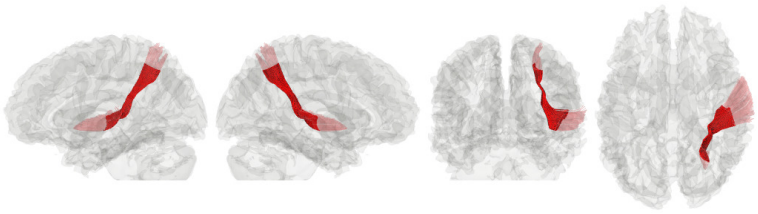

Figure 13: The location of the tract within the brain

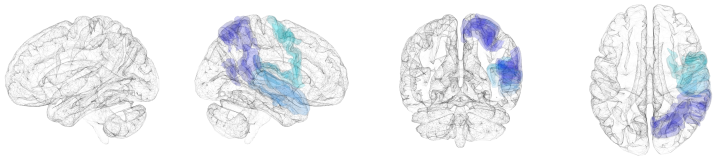

Figure 14: The anatomical areas connected to this tract.

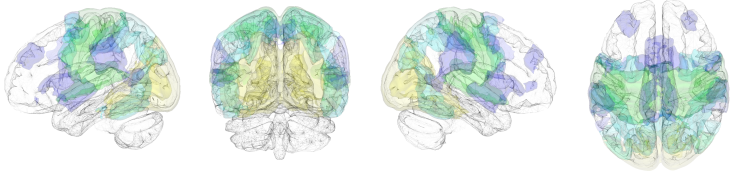

Figure 15: The cortical areas that belong to the functional networks connected to this tract.

4.10 Middle Longitudinal Fasciculus Right Metrics

The DWI metrics as a function of distance along the tract. Significant increases above the control mean for the test subject are shown shaded in yellow and significant decreases are shown in red. To the right of each subplot is the mean and confidence limit of the control data for the whole tract (black) and the mean of the whole tract for the referred individual (red)
Please note that the direction of what is meant by axial and radial is a function of the orientation of the tract within the brain and may vary along the tract. It should also be noted that some tracts end in the spinal cord and this is not shown in these figures.

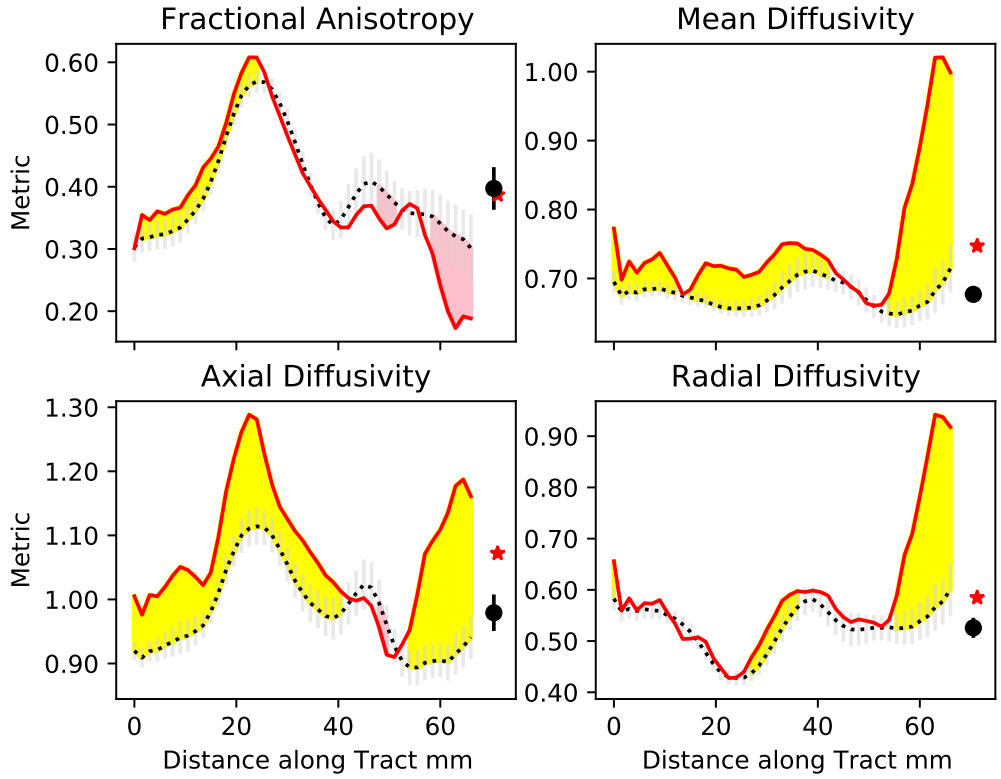

4.11 Corticospinal Tract Right Anatomy

This page shows the relationship between the white matter tract, the cortical areas it is connected to and the functional network that the cortical regions belong to.

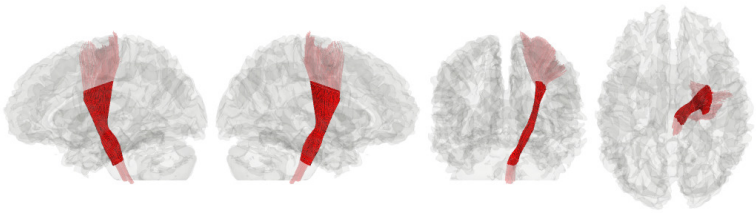

Figure 16: The location of the tract within the brain

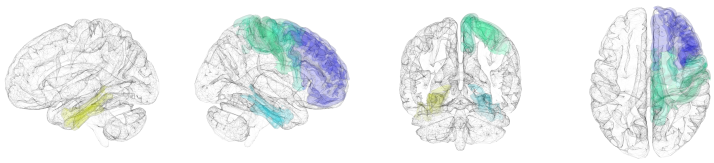

Figure 17: The anatomical areas connected to this tract.

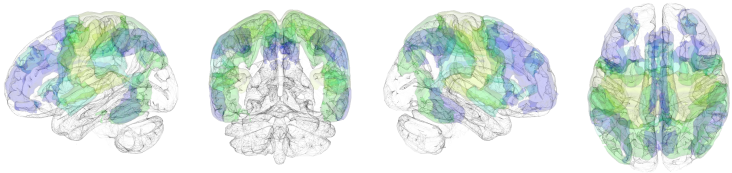

Figure 18: The cortical areas that belong to the functional networks connected to this tract.

4.12 Corticospinal Tract Right Metrics

The DWI metrics as a function of distance along the tract. Significant increases above the control mean for the test subject are shown shaded in yellow and significant decreases are shown in red. To the right of each subplot is the mean and confidence limit of the control data for the whole tract (black) and the mean of the whole tract for the referred individual (red)
Please note that the direction of what is meant by axial and radial is a function of the orientation of the tract within the brain and may vary along the tract. It should also be noted that some tracts end in the spinal cord and this is not shown in these figures.

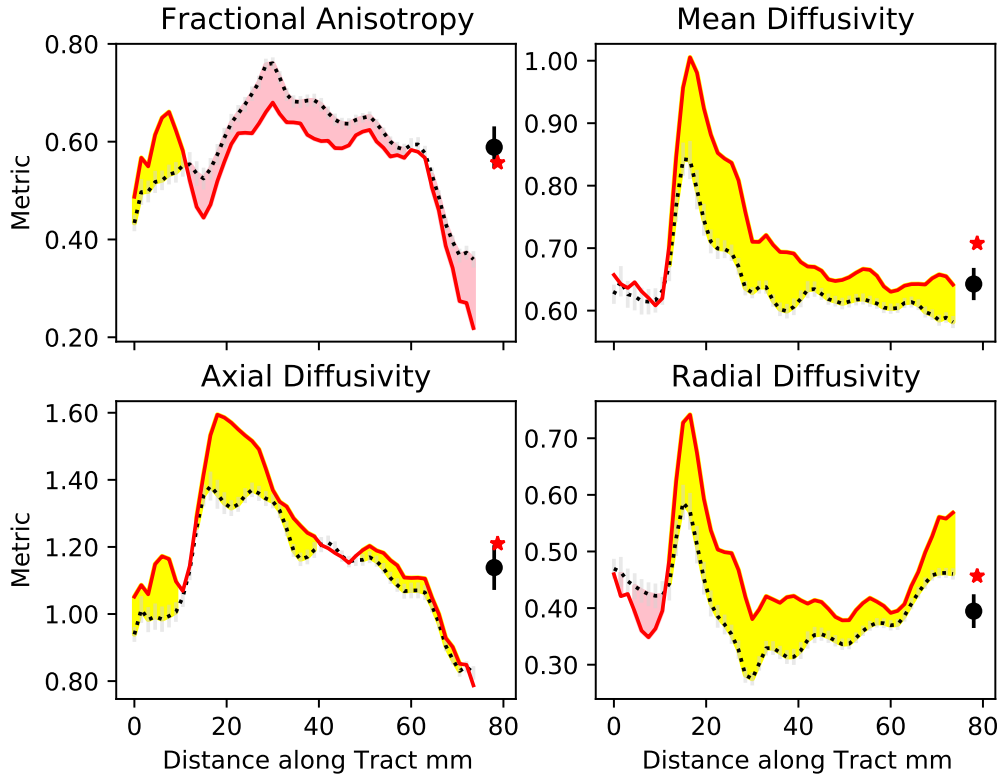

4.13 Dentatorubrothalamic Tract Right Anatomy

This page shows the relationship between the white matter tract, the cortical areas it is connected to and the functional network that the cortical regions belong to.

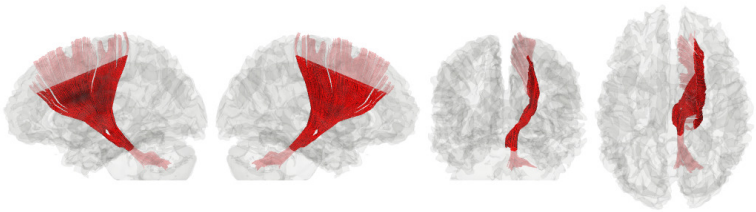

Figure 19: The location of the tract within the brain

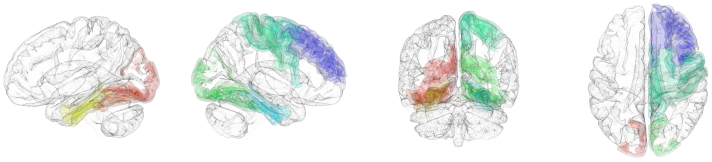

Figure 20: The anatomical areas connected to this tract.

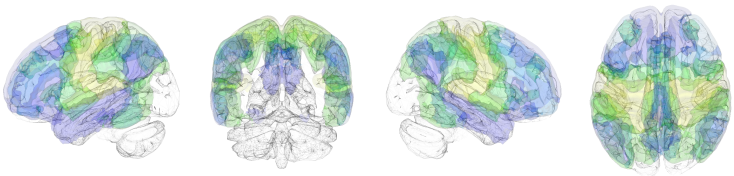

Figure 21: The cortical areas that belong to the functional networks connected to this tract.

4.14 Dentatorubrothalamic Tract Right Metrics

The DWI metrics as a function of distance along the tract. Significant increases above the control mean for the test subject are shown shaded in yellow and significant decreases are shown in red. To the right of each subplot is the mean and confidence limit of the control data for the whole tract (black) and the mean of the whole tract for the referred individual (red)
Please note that the direction of what is meant by axial and radial is a function of the orientation of the tract within the brain and may vary along the tract. It should also be noted that some tracts end in the spinal cord and this is not shown in these figures.

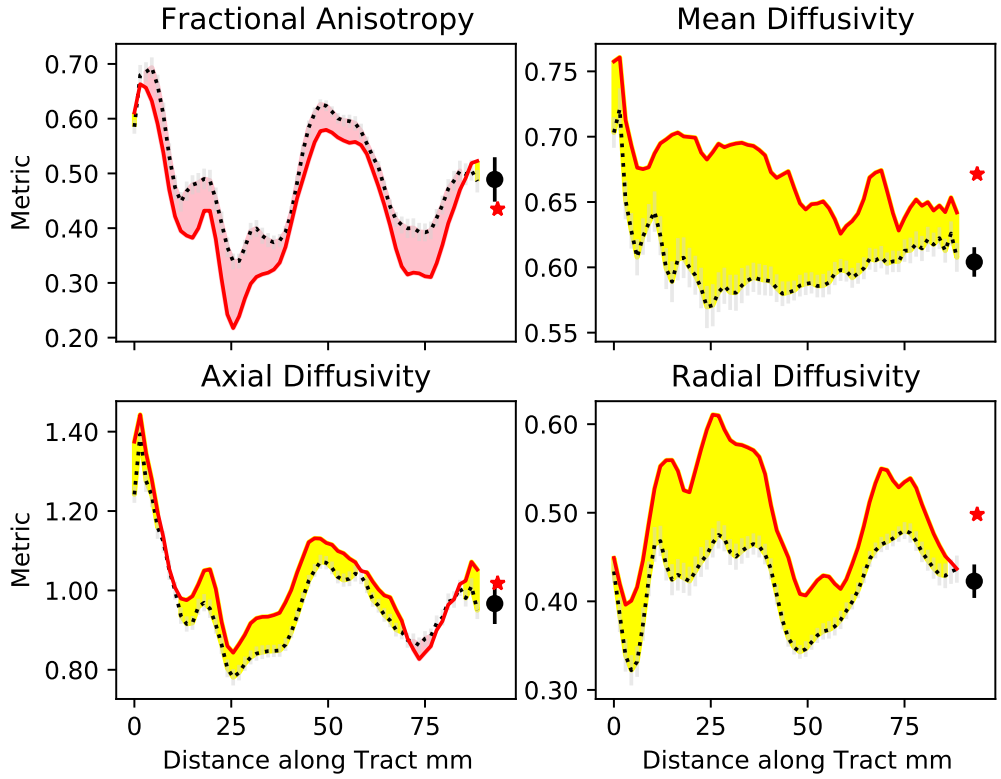

4.15 Frontal Aslant Tract Right Anatomy

This page shows the relationship between the white matter tract, the cortical areas it is connected to and the functional network that the cortical regions belong to.

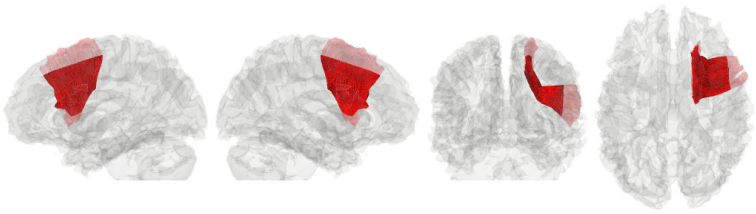

Figure 22: The location of the tract within the brain

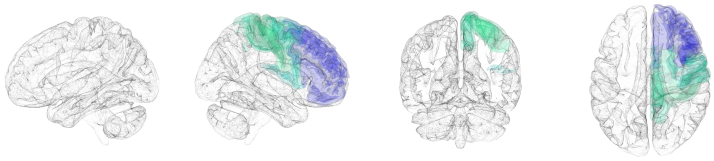

Figure 23: The anatomical areas connected to this tract.

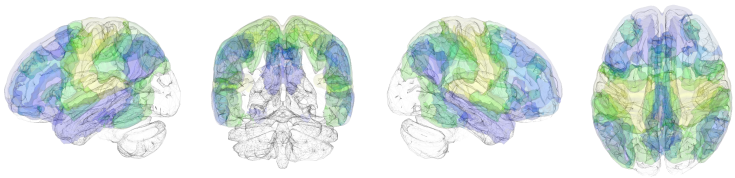

Figure 24: The cortical areas that belong to the functional networks connected to this tract.

4.16 Frontal Aslant Tract Right Metrics

The DWI metrics as a function of distance along the tract. Significant increases above the control mean for the test subject are shown shaded in yellow and significant decreases are shown in red. To the right of each subplot is the mean and confidence limit of the control data for the whole tract (black) and the mean of the whole tract for the referred individual (red)
Please note that the direction of what is meant by axial and radial is a function of the orientation of the tract within the brain and may vary along the tract. It should also be noted that some tracts end in the spinal cord and this is not shown in these figures.

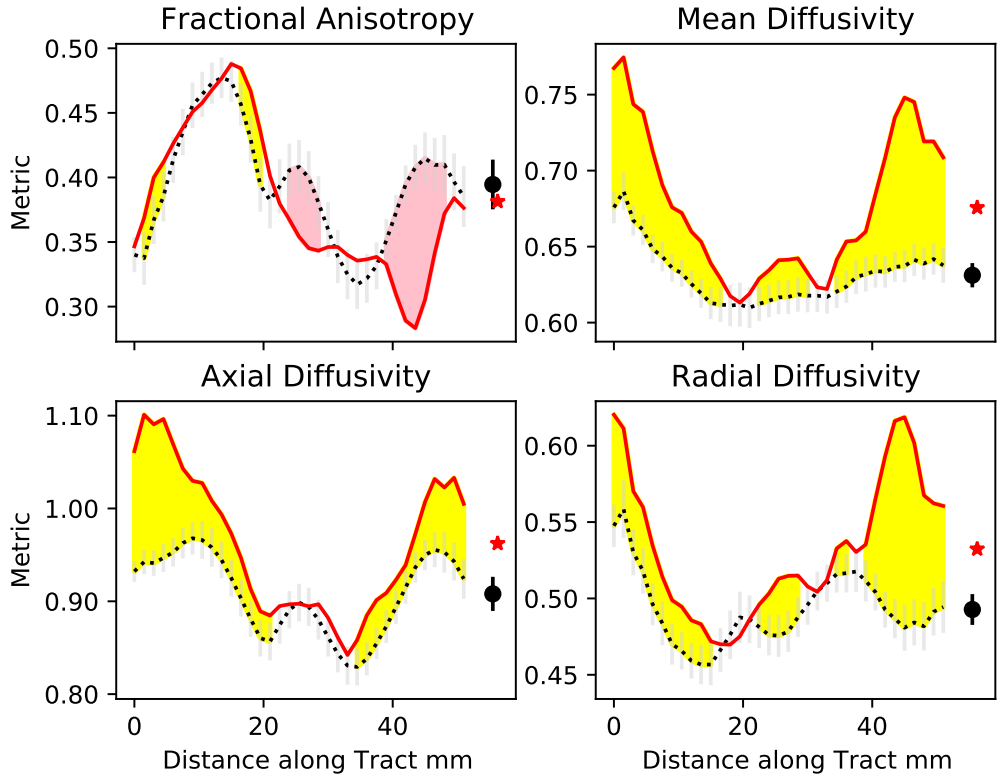

4.17 Corticostriatal Pathway Superior Left Anatomy

This page shows the relationship between the white matter tract, the cortical areas it is connected to and the functional network that the cortical regions belong to.

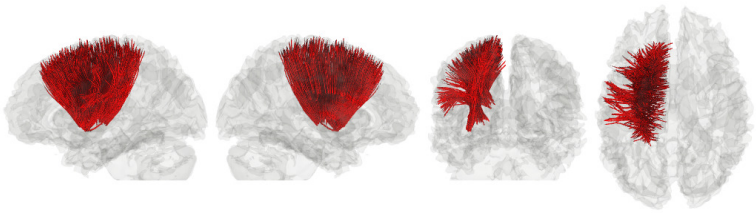

Figure 25: The location of the tract within the brain

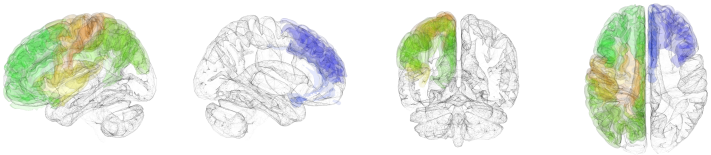

Figure 26: The anatomical areas connected to this tract.

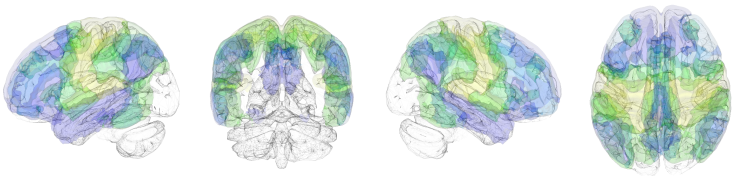

Figure 27: The cortical areas that belong to the functional networks connected to this tract.

4.18 Corticostriatal Pathway Superior Left Metrics

The DWI metrics as a function of distance along the tract. Significant increases above the control mean for the test subject are shown shaded in yellow and significant decreases are shown in red. To the right of each subplot is the mean and confidence limit of the control data for the whole tract (black) and the mean of the whole tract for the referred individual (red)
Please note that the direction of what is meant by axial and radial is a function of the orientation of the tract within the brain and may vary along the tract. It should also be noted that some tracts end in the spinal cord and this is not shown in these figures.

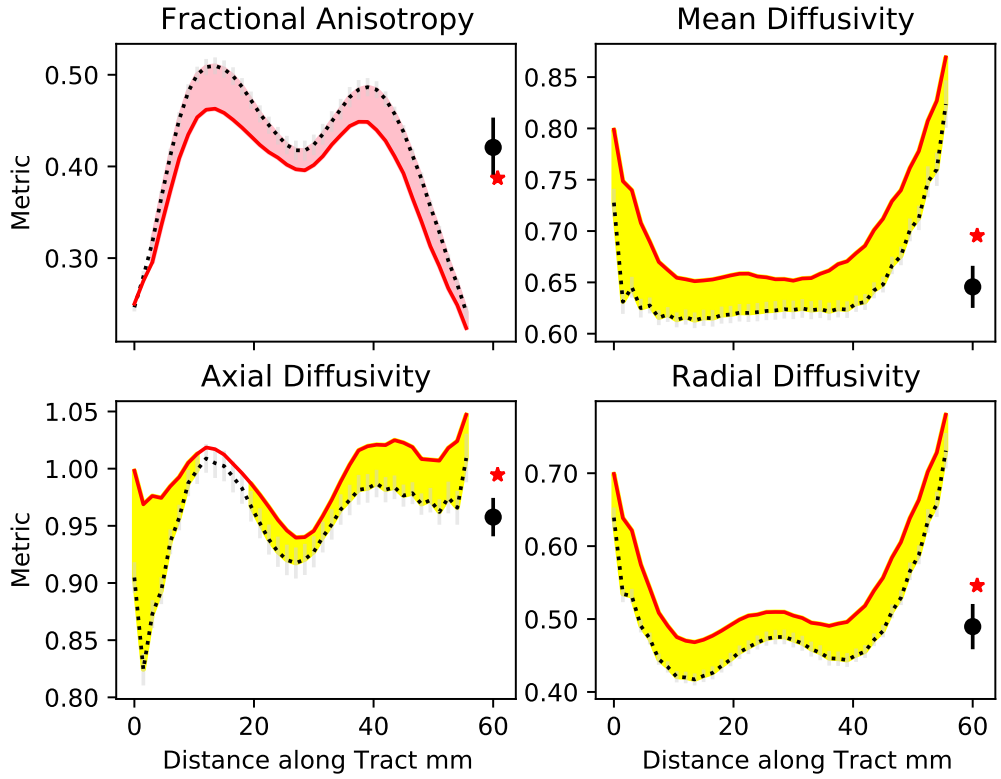

4.19 Superior Longitudinal Fasciculus 2 Right Anatomy

This page shows the relationship between the white matter tract, the cortical areas it is connected to and the functional network that the cortical regions belong to.

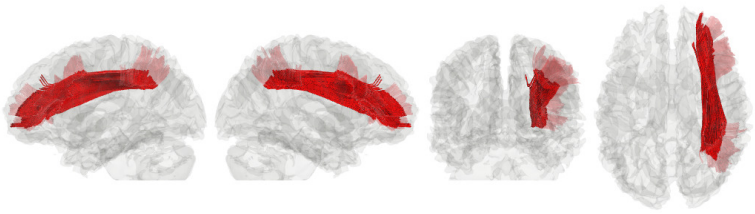

Figure 28: The location of the tract within the brain

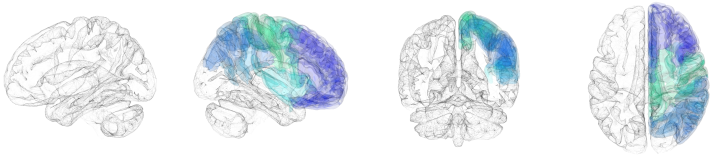

Figure 29: The anatomical areas connected to this tract.

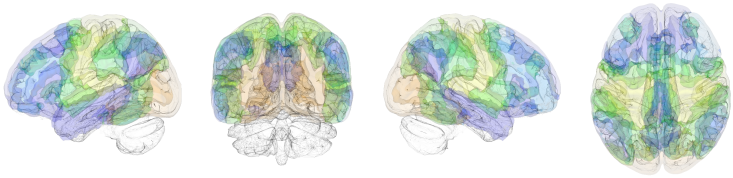

Figure 30: The cortical areas that belong to the functional networks connected to this tract.

4.20 Superior Longitudinal Fasciculus 2 Right Metrics

The DWI metrics as a function of distance along the tract. Significant increases above the control mean for the test subject are shown shaded in yellow and significant decreases are shown in red. To the right of each subplot is the mean and confidence limit of the control data for the whole tract (black) and the mean of the whole tract for the referred individual (red)
Please note that the direction of what is meant by axial and radial is a function of the orientation of the tract within the brain and may vary along the tract. It should also be noted that some tracts end in the spinal cord and this is not shown in these figures.

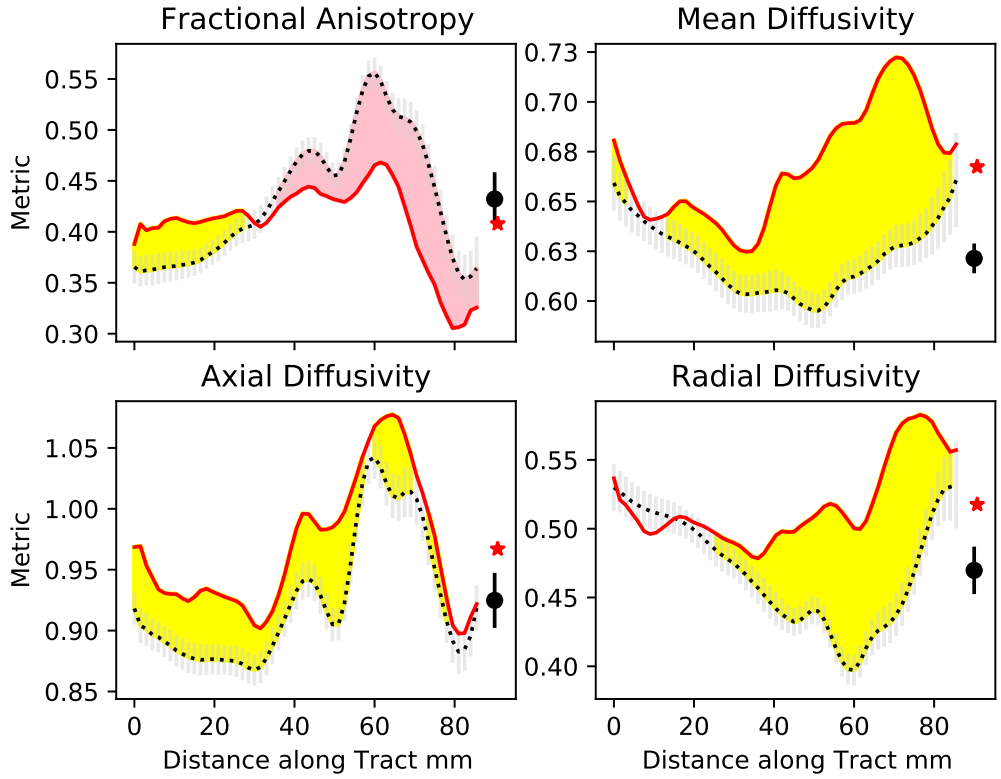

5 Cortical thickness findings

Here we show the statistical map of the significant decreases in cortical thickness as a probability map where the referred individual has been compared to controls. The map has been thresholded at a 1-p value of 0.95. Statistically decreased thickness is shown in yellow. The areas shown are clusters of brain areas, following corrections for multiple comparisons, where the null hypothesis of being the same as the control group has been rejected with a probability of being less than due to chance of less than 5\%.

5.1 Left side decreases in cortical thickness

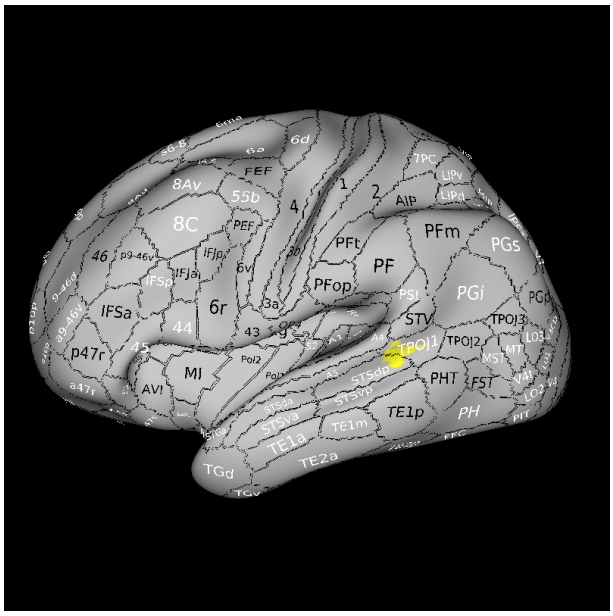

Figure 31: Left lateral view

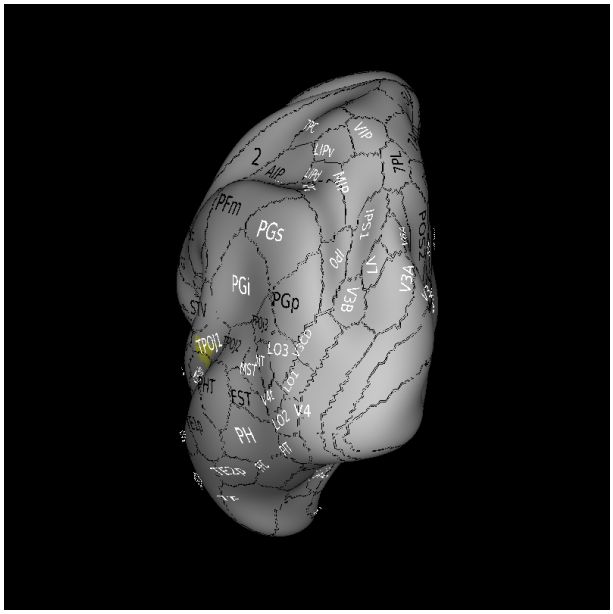

Figure 32: Left posterior view

5.2 Left side decreases in cortical thickness overlaid onto YEO functional networks

The networks are coloured as follows:

Network	Colour
Purple	Visual
Blue	Somatosensory/Motor
Green	Dorsal Attention
Violet	Visual Attention
Cream	Visual Limbic
Orange	Frontoparietal
Red	Visual Default

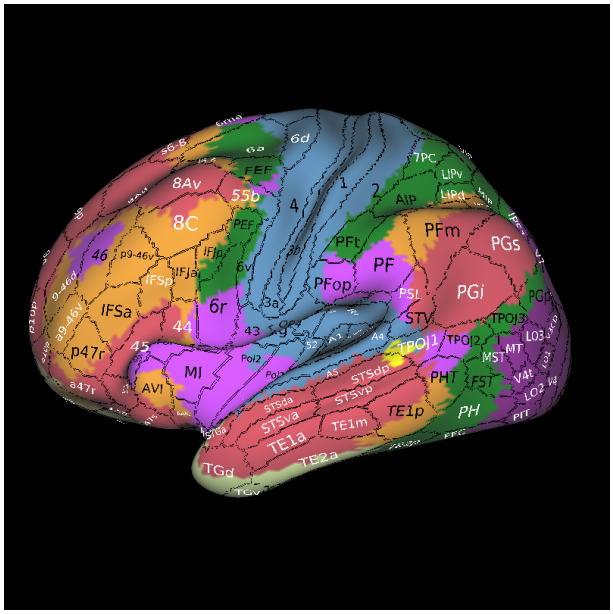

Figure 33: Left lateral view

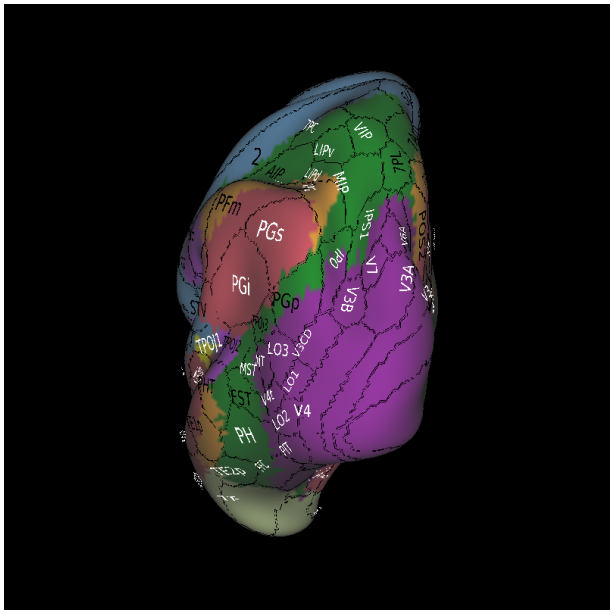

Figure 34: Left posterior view

6 Cortical myelin findings

Here we show the statistical map of the significant decreases in cortical myelin as a probability map where the referred individual has been compared to controls. The map has been thresholded at a 1-p value of 0.95. Statistically decreased myelin is shown in yellow. The areas shown are clusters of brain areas, following corrections for multiple comparisons, where the null hypothesis of being the same as

the control group has been rejected with a probability of being less than due to chance of less than 5\%.

6.1 Left side decreases in cortical myelin

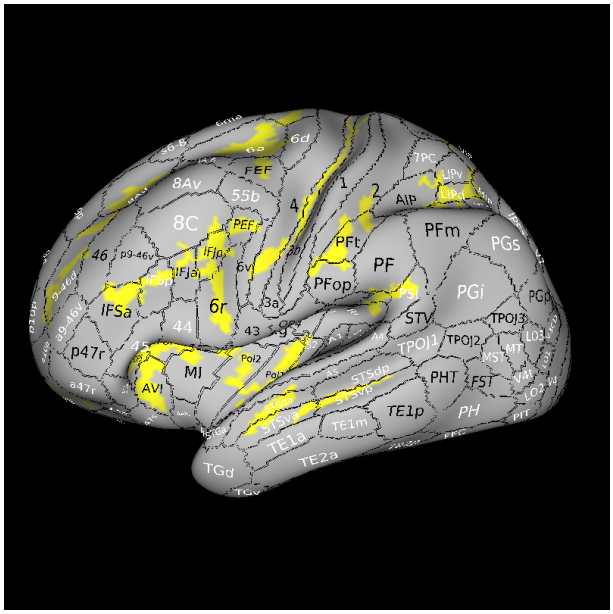

Figure 35: Left lateral view

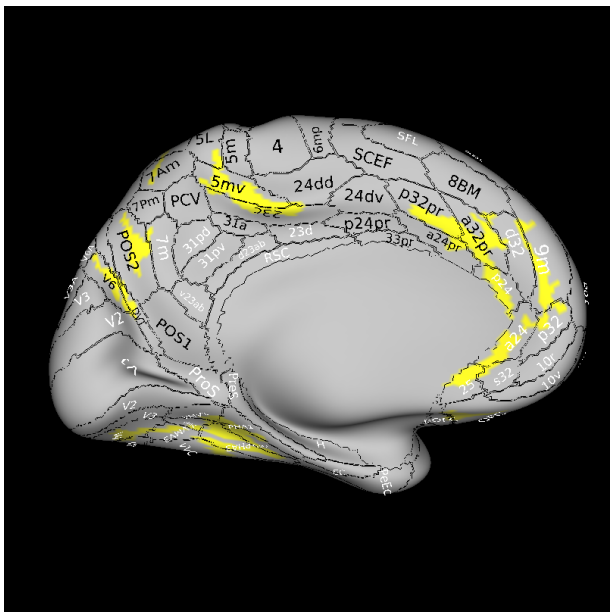

Figure 36: Left medial view

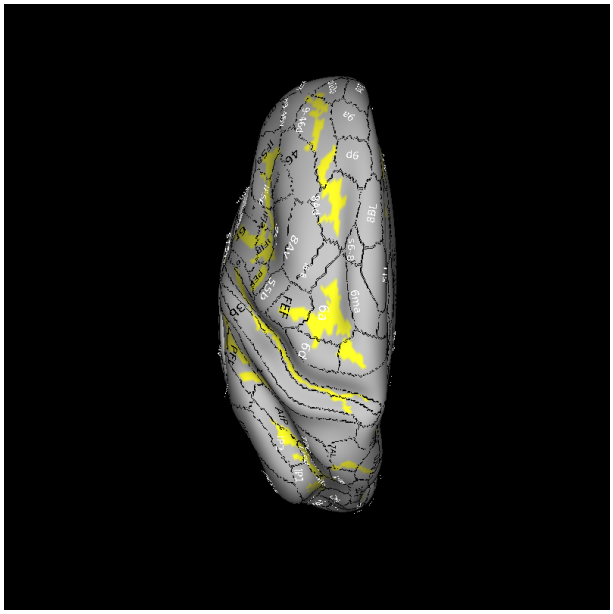

Figure 37: Left superior view

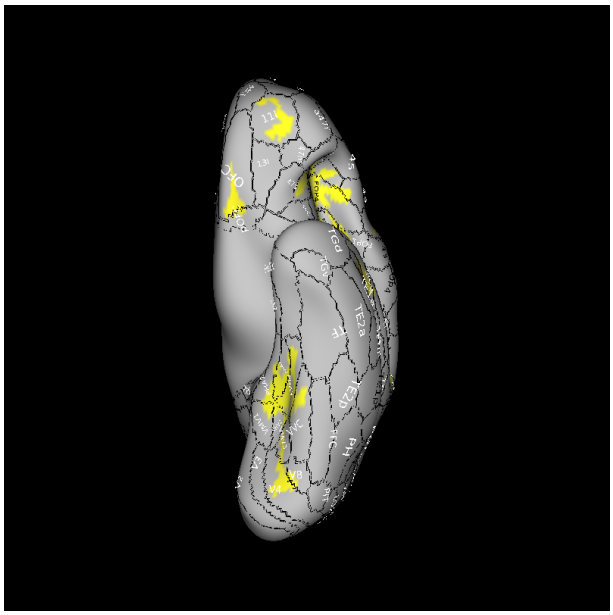

Figure 38: Left inferior view

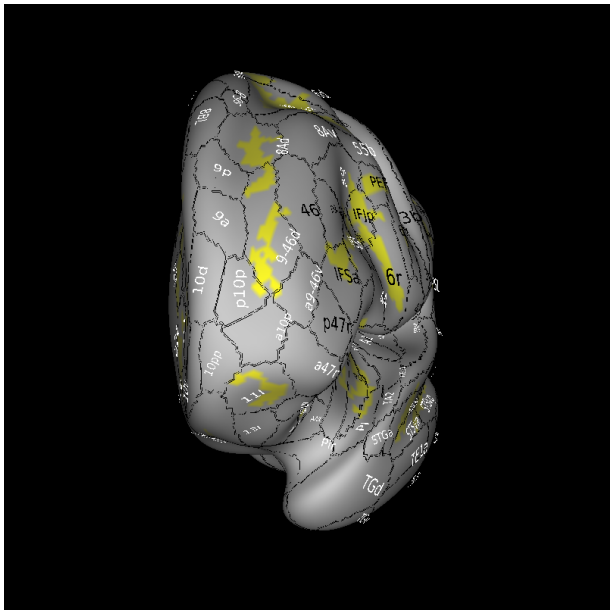

Figure 39: Left anterior view

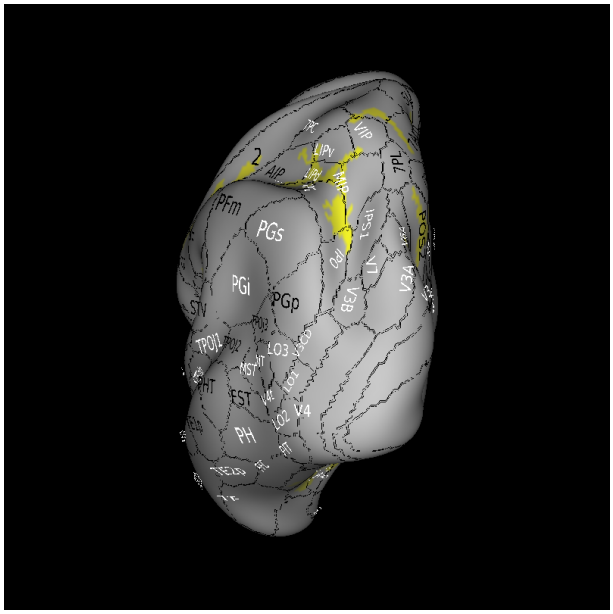

Figure 40: Left posterior view

6.2 Right side decreases in cortical myelin

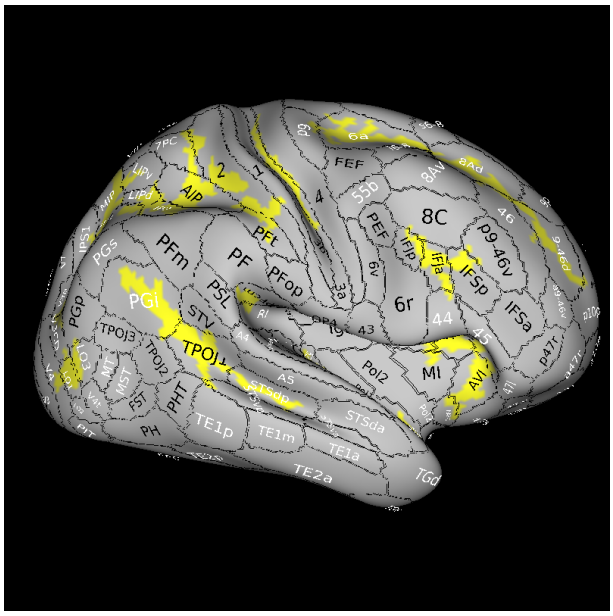

Figure 41: Right lateral view

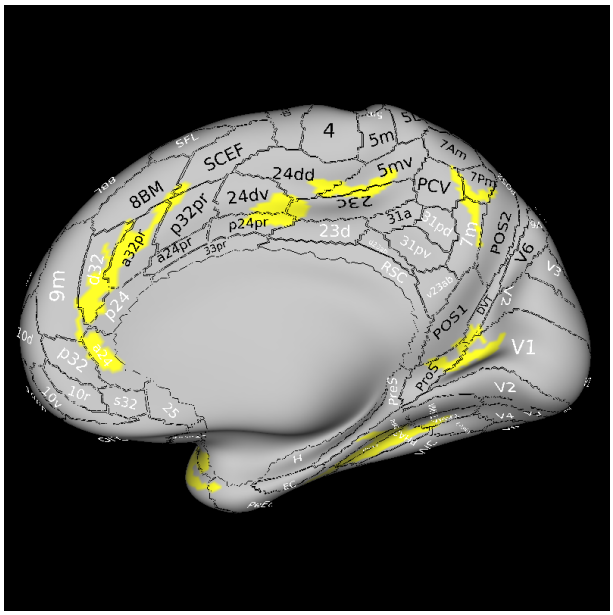

Figure 42: Right medial view

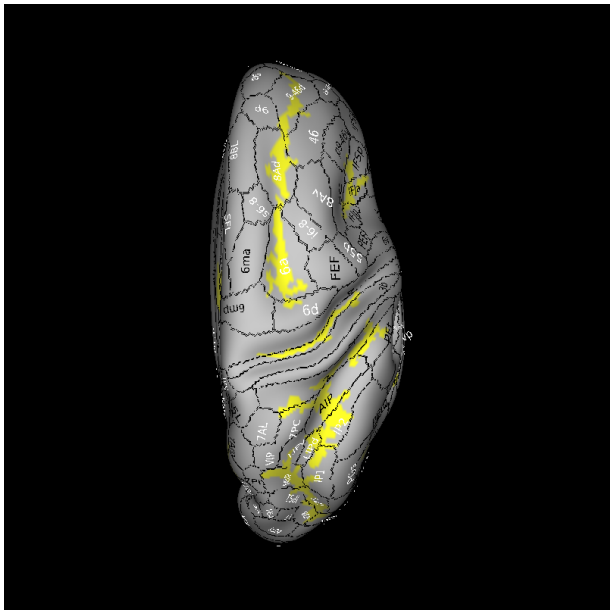

Figure 43: Right superior view

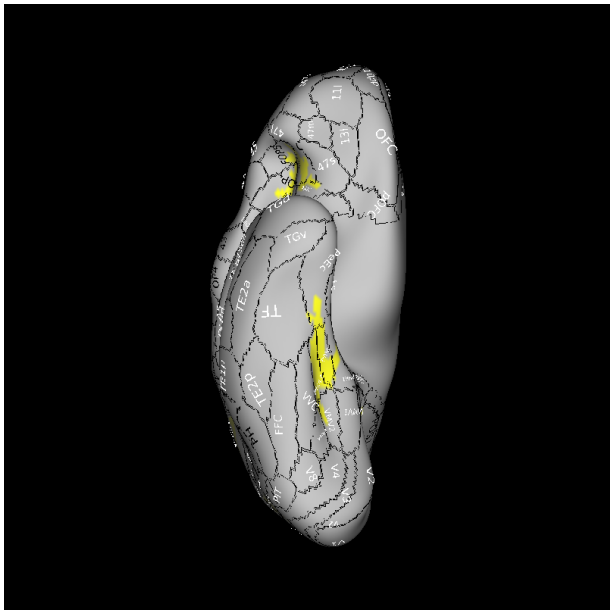

Figure 44: Right inferior view

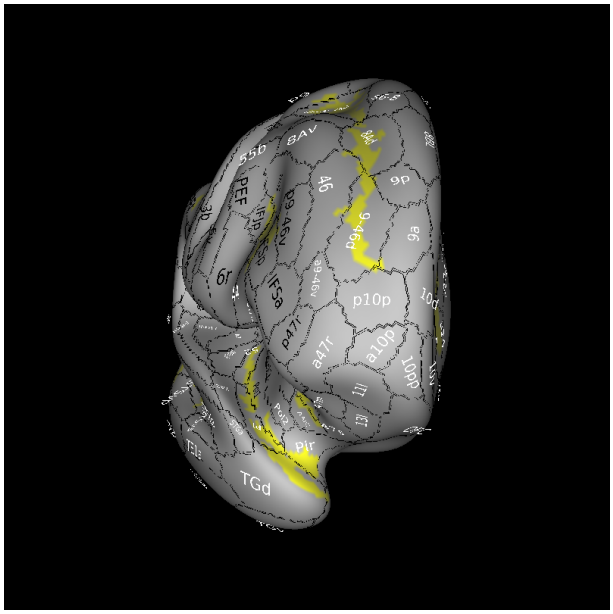

Figure 45: Right anterior view

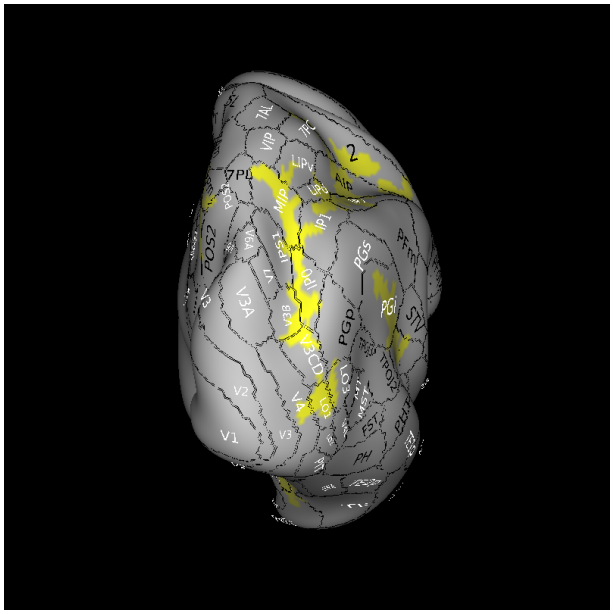

Figure 46: Right posterior view

6.3 Left side decreases in cortical myelin overlaid onto YEO functional networks

The networks are coloured as follows:

Network	Colour
Purple	Visual
Blue	Somatosensory/Motor
Green	Dorsal Attention
Violet	Visual Attention
Cream	Visual Limbic
Orange	FrontoParietal
Red	Visual Default

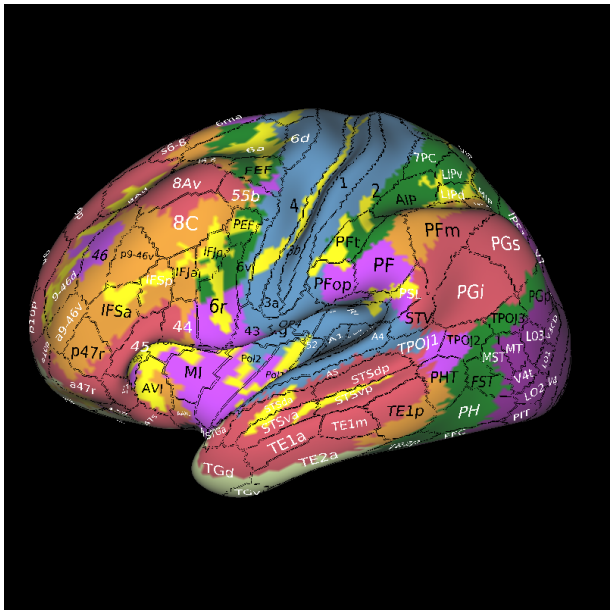

Figure 47: Left lateral view

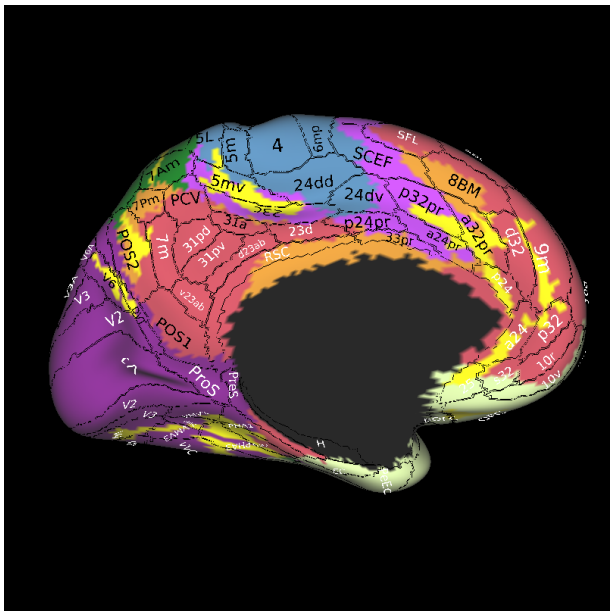

Figure 48: Left medial view

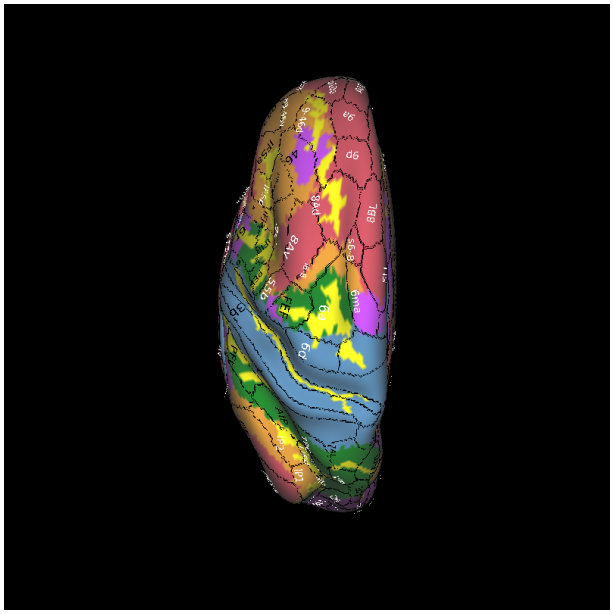

Figure 49: Left superior view

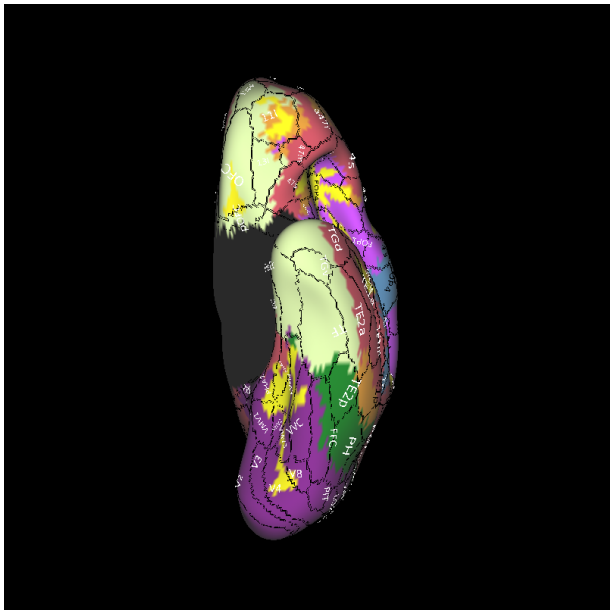

Figure 50: Left inferior view

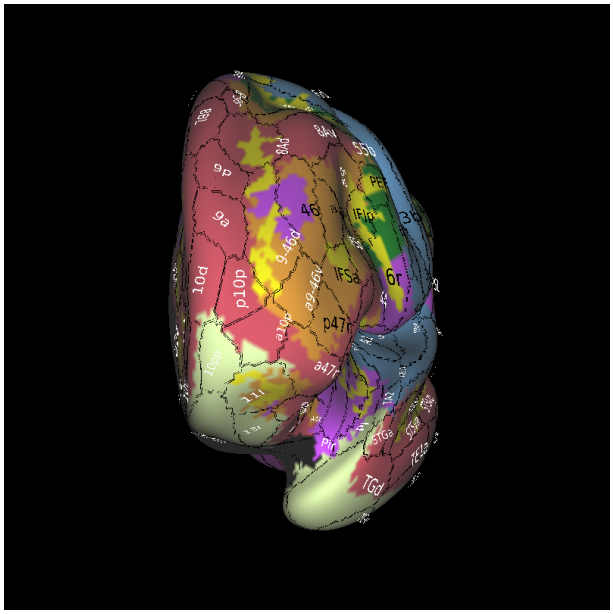

Figure 51: Left anterior view

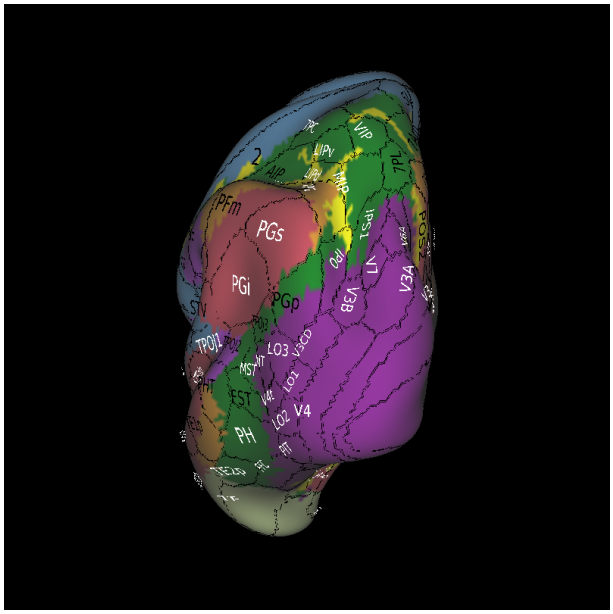

Figure 52: Left posterior view

6.4 Right side decreases in cortical myelin overlaid onto YEO functional networks

The networks are coloured as follows:

Network	Colour
Purple	Visual
Blue	Somatosensory/Motor
Green	Dorsal Attention
Violet	Visual Attention
Cream	Visual Limbic
Orange	FrontoParietal
Red	Visual Default

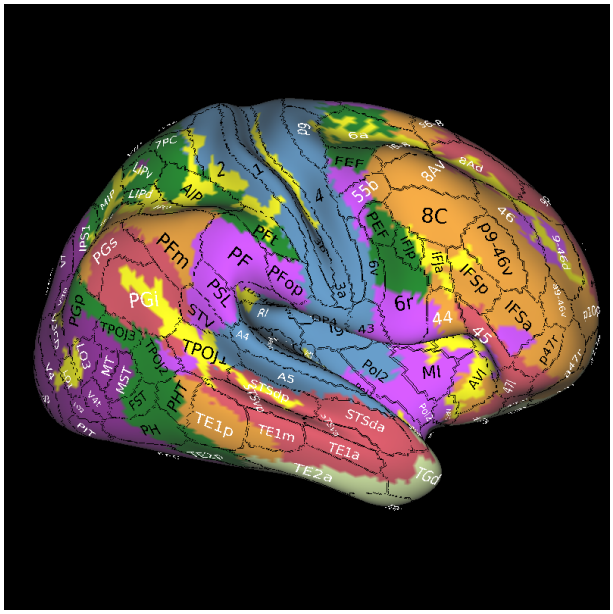
8C
p9-46v
IFSp
IFSa
6r
44
45
Pol2
MI
PFm
PF
PFop
PGi
PGs
PGp
STV
PSL
TPOJ1
TPOJ3
MT
MST
FST
PH
TE1p
TE1m
TE1a
TE2a
STSda
TGd
PFt
PBelt
LBelt
MBelt
A1
A4
A5
RI
52
PeriSylv
6v
6mp
6a
55b
FEF
8Av
8Ad
8BL
9p
9-46d
i6-8
s6-8
SFL
AIP
7PC
LIPv
LIPd
VIP
MIP
PGi
PGs
PGp
TPOJ3
TPOJ1
STV
PSL
PFm
PF
PFop
PFt
PH
MT
MST
FST
V4t
V3A
V3B
V4
V8
PIT
FFC
VVC
PHA1
PHA2
PHA3
TE1p
TE1m
TE1a
TE2a
TGd
STSda
STSdp
A5
RI
PBelt
LBelt
MBelt
A1
A4
52
PeriSylv
Pol2
MI
6r
44
45
IFSa
IFSp
p9-46v
8C
8Av
8Ad
8BL
9p
9-46d
46
SFL
55b
FEF
6a
6v
6mp
i6-8
s6-8
AIP
7PC
LIPv
LIPd
VIP
MIP
2
1
3a
3b
4
43
OP4
OP1
OP2-3
A4
A5
RI
PeriSylv
Ig
Pol2
MI
6r
44
45
IFSa
p47r
a47r
11l
13l
47l
47m
a47r
IFSp
IFSa
p9-46v
8C
8Av
8Ad
8BL
9p
9-46d
46
SFL
55b
FEF
6a
6v
6mp
6d
i6-8
s6-8
AIP
7PC
LIPv
LIPd
VIP
MIP
2
1
3a
3b
4
43
OP4
OP1
OP2-3
A4
A5
RI
PeriSylv
Ig
Pol2
MI
6r
44
45
IFSa
IFSp

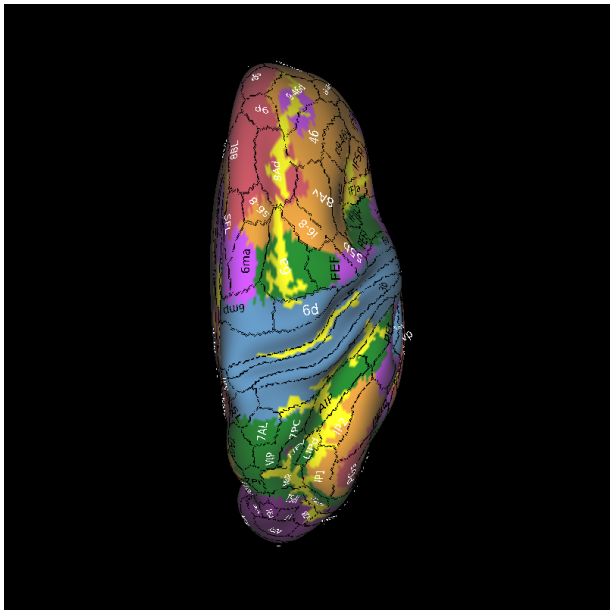

Figure 55: Right superior view

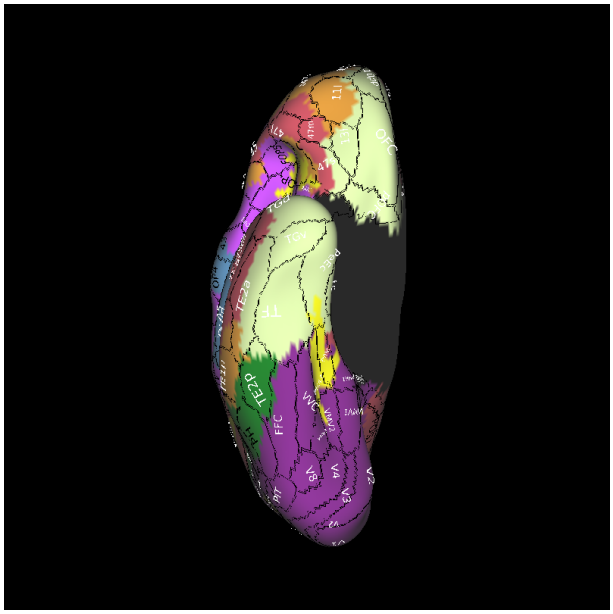

Figure 56: Right inferior view

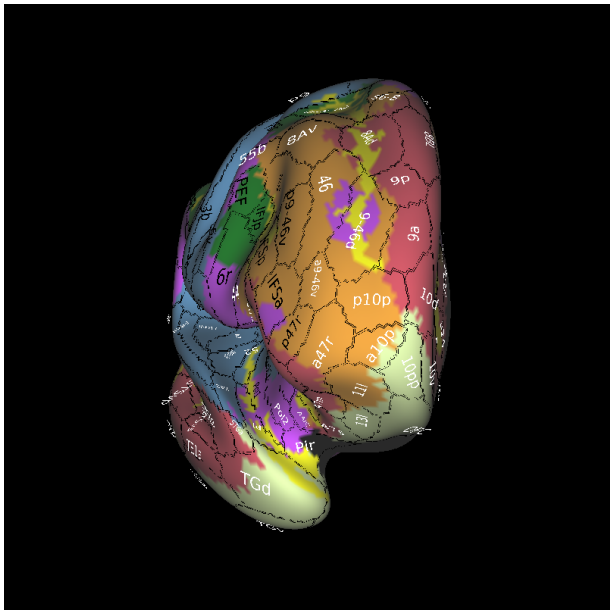

Figure 57: Right anterior view

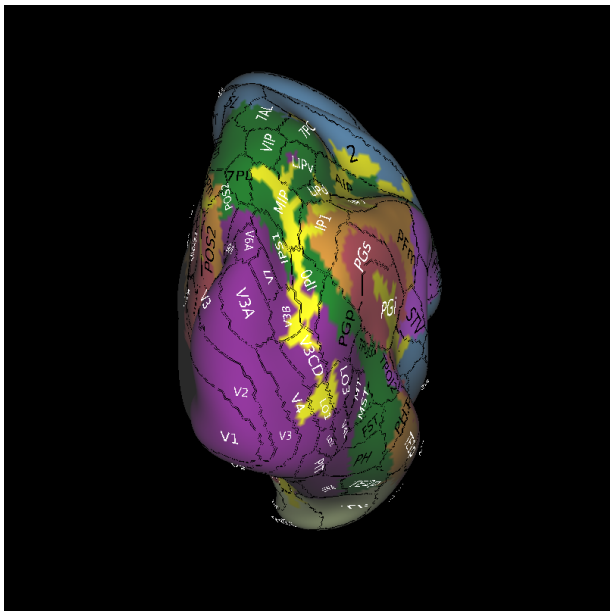

Figure 58: Right posterior view

Here we show the statistical map of the significant increases in cortical myelin as a probability map where the referred individual has been compared to controls. The map has been thresholded at a 1-p value of 0.95. Statistically decreased myelin is shown in yellow. The areas shown are clusters of brain areas, following corrections for multiple comparisons, where the null hypothesis of being the same as the control group has been rejected with a probability of being less than due to chance of less than 5\%.

6.5 Left side increases in cortical myelin

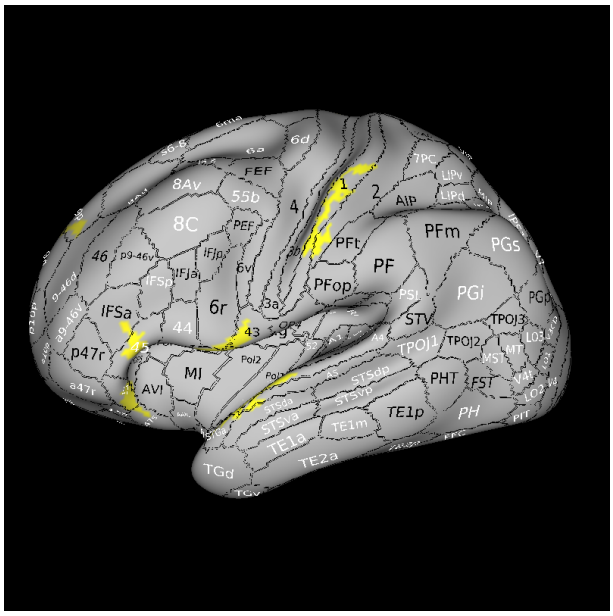

Figure 59: Left lateral view

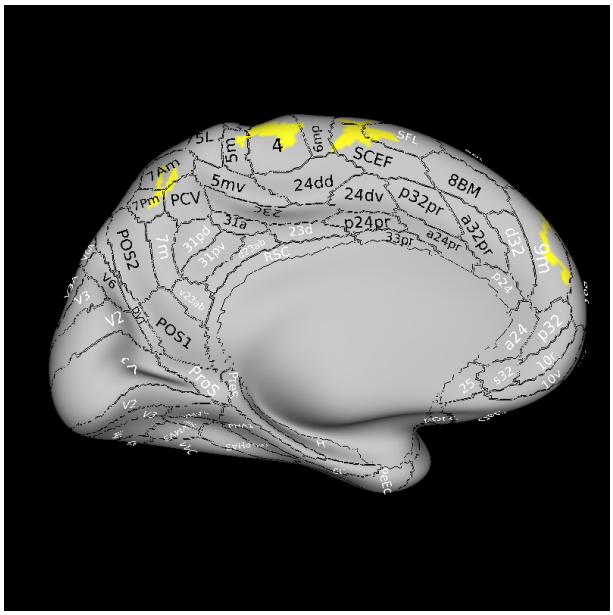

Figure 60: Left medial view

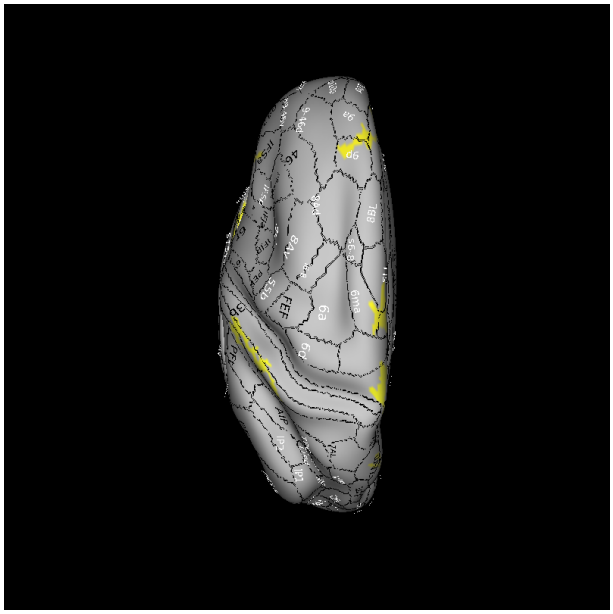

Figure 61: Left superior view

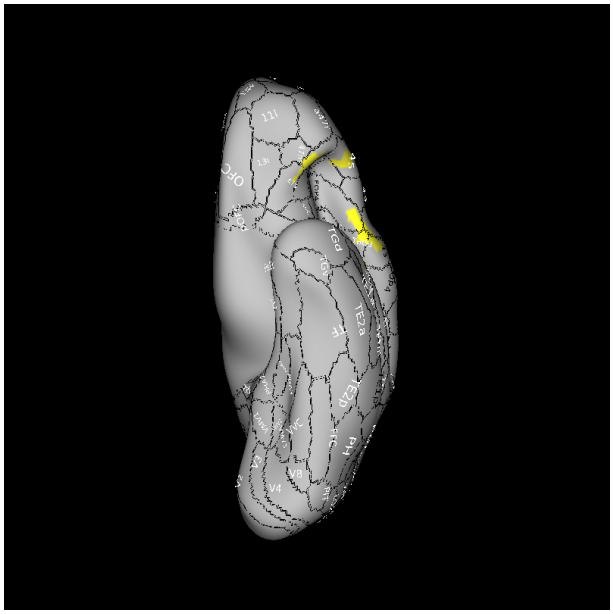

Figure 62: Left inferior view

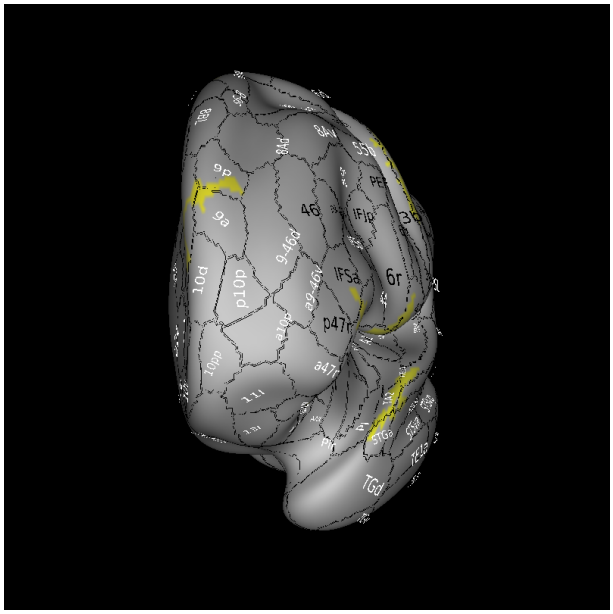

Figure 63: Left anterior view

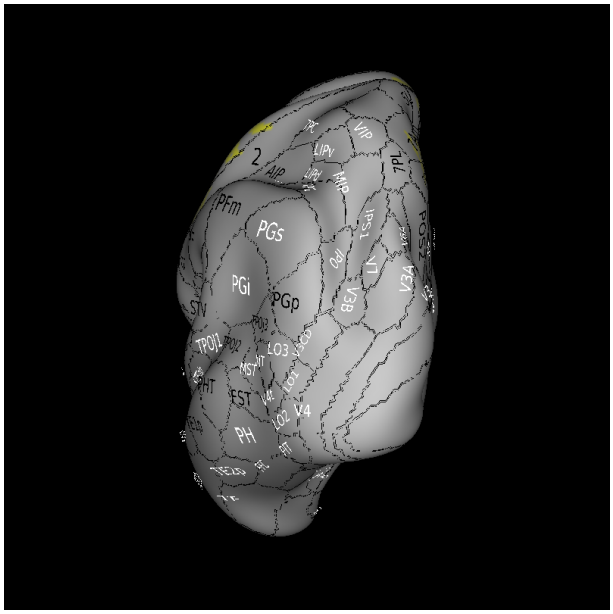

Figure 64: Left posterior view

6.6 Right side increases in cortical myelin

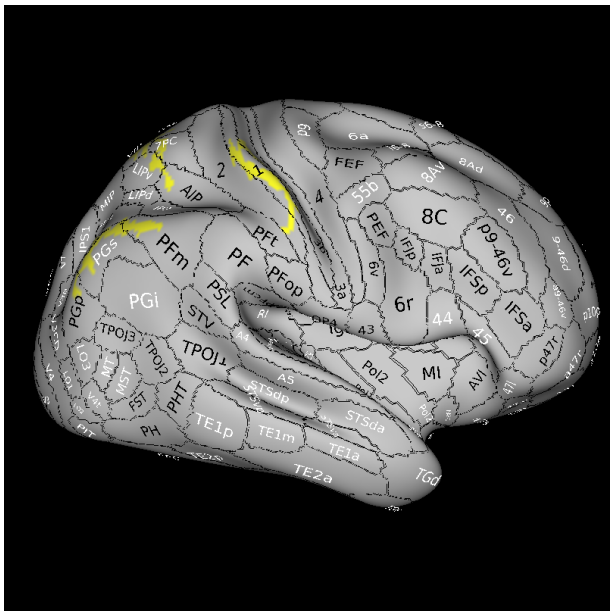

Figure 65: Right lateral view

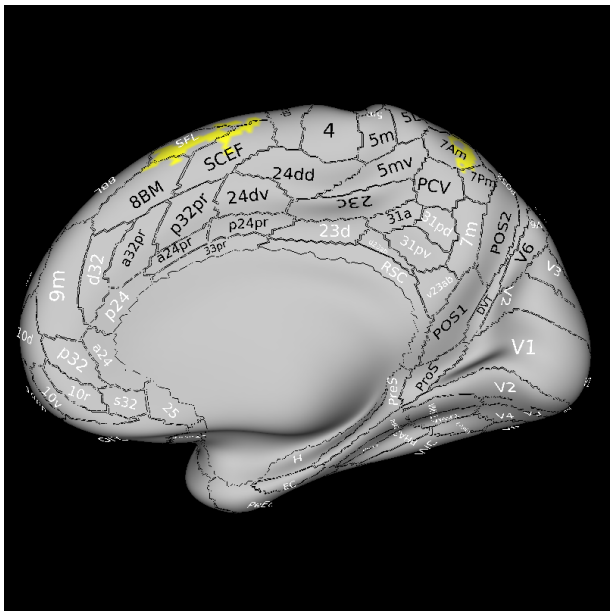

Figure 66: Right medial view

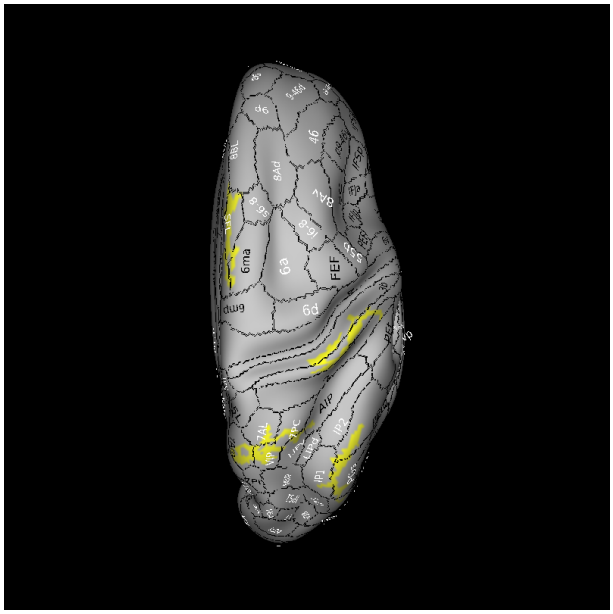

Figure 67: Right superior view

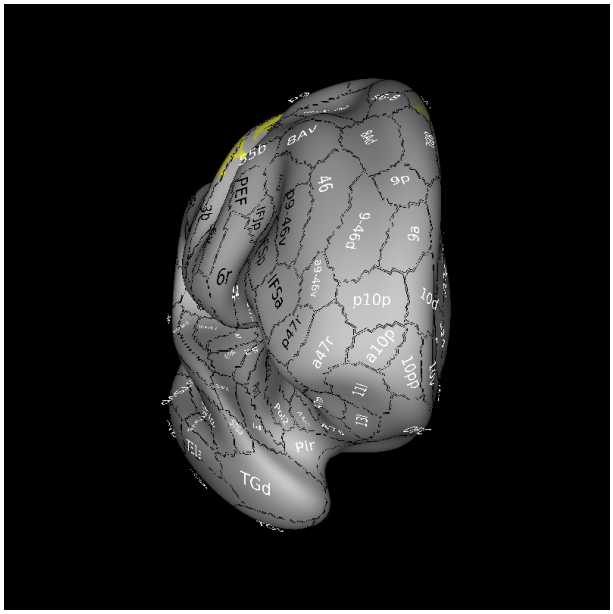

Figure 68: Right anterior view

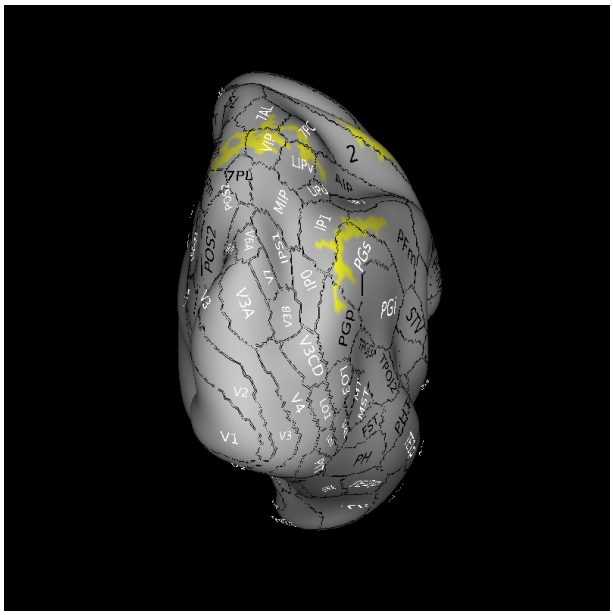

Figure 69: Right posterior view

6.7 Left side increases in cortical myelin overlaid onto YEO functional networks

The networks are coloured as follows:

Network	Colour
Purple	Visual
Blue	Somatosensory/Motor
Green	Dorsal Attention
Violet	Visual Attention
Cream	Visual Limbic
Orange	FrontoParietal
Red	Visual Default

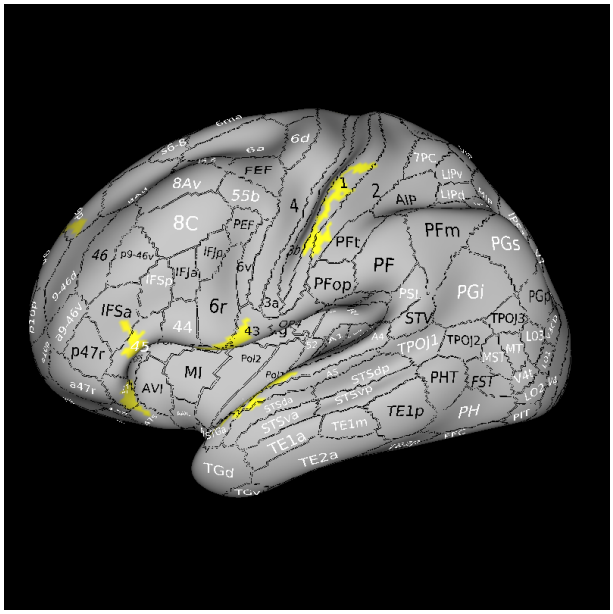

Figure 70: Left lateral view

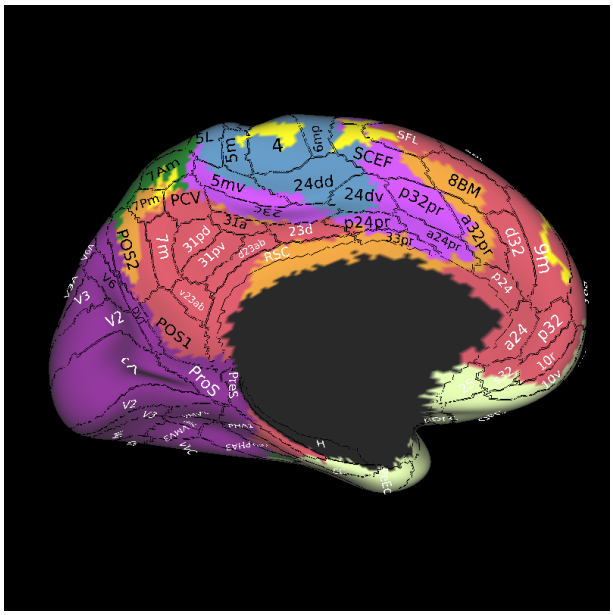

Figure 71: Left medial view

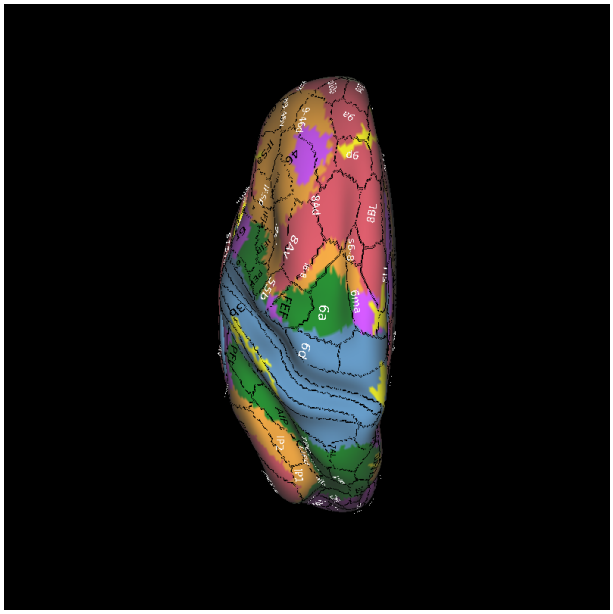

Figure 72: Left superior view

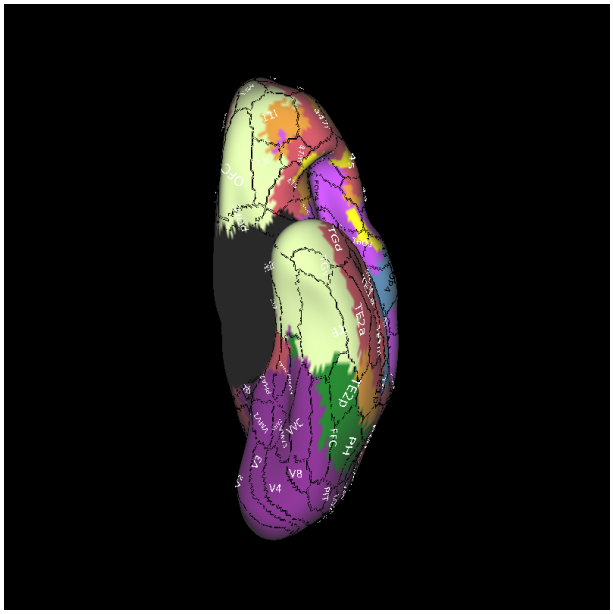

Figure 73: Left inferior view

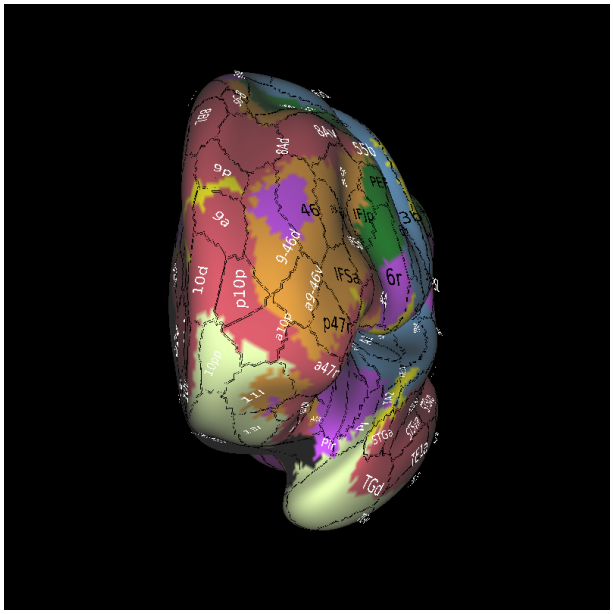

Figure 74: Left anterior view

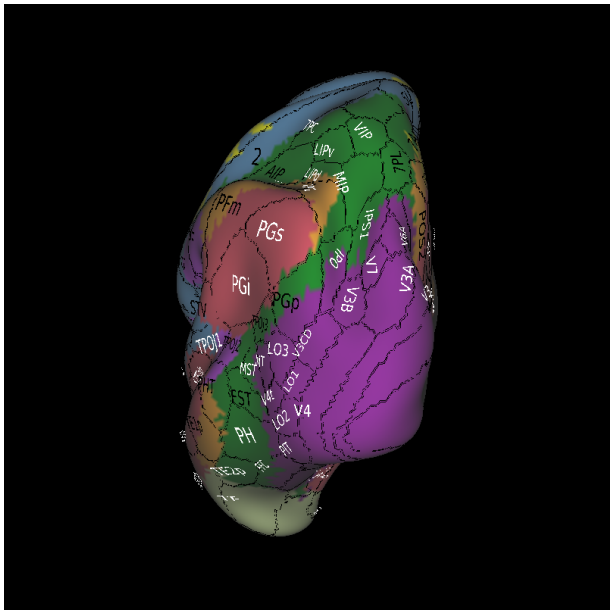

Figure 75: Left posterior view

6.8 Right side increases in cortical myelin overlaid onto YEO functional networks

The networks are coloured as follows:

Network	Colour
Purple	Visual
Blue	Somatosensory/Motor
Green	Dorsal Attention
Violet	Visual Attention
Cream	Visual Limbic
Orange	FrontoParietal
Red	Visual Default

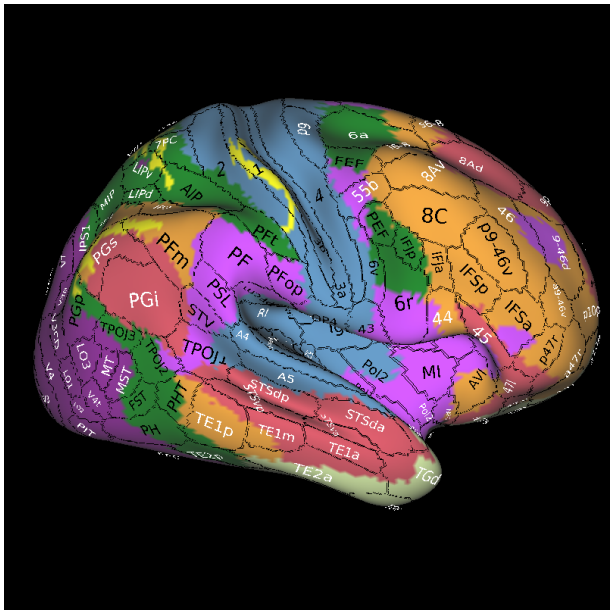

Figure 76: Right lateral view

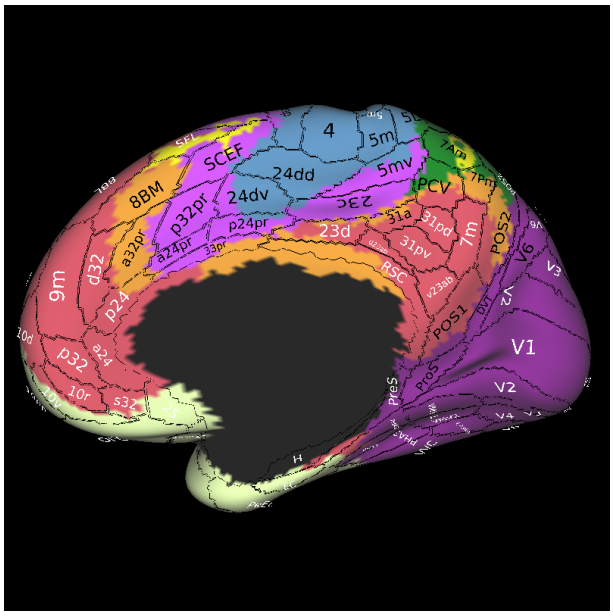

Figure 77: Right medial view

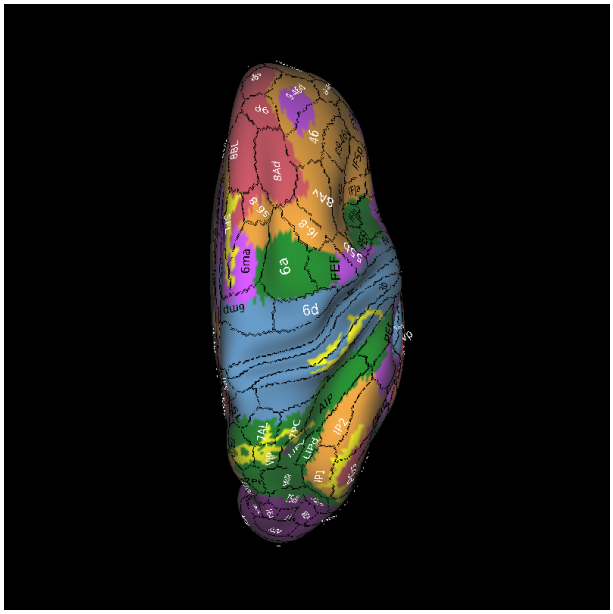

Figure 78: Right superior view

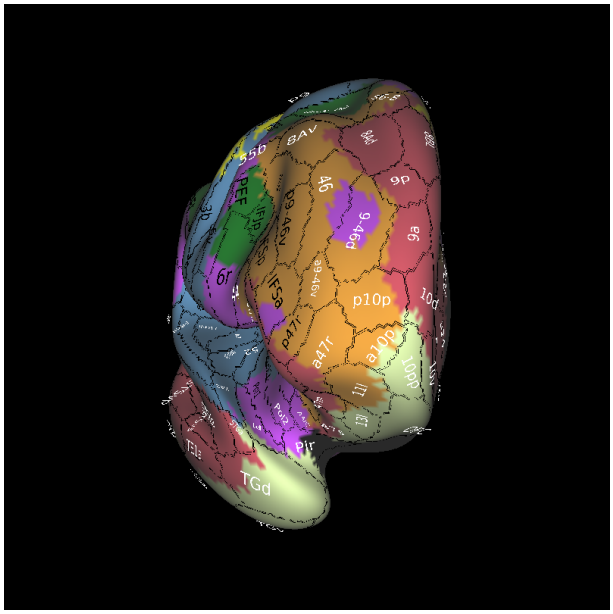

Figure 79: Right anterior view

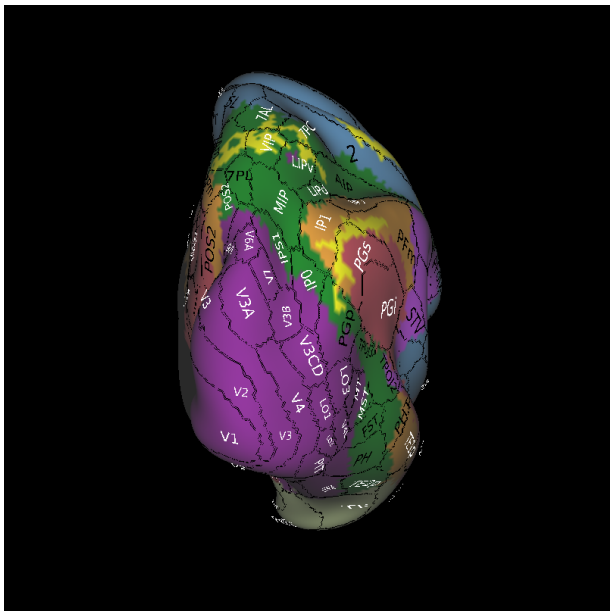

Figure 80: Right posterior view

7 Biographies of the authors of this document

7.1 Professor G. Green

Gary Green was the founding Director of the York Neuroimaging Centre, York, UK and a Professor of Neuroimaging at the University of York from January 2004 until September 2017. This Centre provided access for clinicians and academics to use MRI, MEG, TMS, EEG, EOG and Psychophysics for the collection of data for both clinical use and fundamental research. It also provided access to high performance computing for the analysis of neuroimaging data. The Centre provided training for undergraduates, postgraduates, medical graduates and visiting academics. He was also Director of the York Diagnostic Imaging Centre, providing a clinical service for the MRI and MEG scanning of patients. Professor Green was the founding co-director of the Centre for Hyperpolarisation in Magnetic Resonance in York and a MRC funded National Centre for MRI Research in Leeds.
He holds the degrees of MA DPhil BM BCh from Oxford University where he was also an EP Abrahams Fellow at Hertford College.
He was the vice-chairman of the Wellcome Trust Neuroscience and Mental Health panel.
He has acted as an advisor to the UK MRC, EPSRC, BBSRC, the Wellcome Trust, the German Helmholtz Association, the US NIH, the Scottish SINAPSE consortium of University Neuroimaging Centres and to other government agencies.
He was a member of the Court of the Royal College of Surgeons, England.
Prior to working at the University of York he was the Director of the Institute of Neuroscience at the University of Newcastle upon Tyne and a Reader at Newcastle Medical School and University.
He has published more than 150 academic articles. Full details can be found at
https://www.innovision-ip.co.uk/the-team/gary-green/
He was a founding Director of York Instruments Ltd which won the Institute of Physics Innovation Award for a Startup Company in 2018.
In 2017 he was the Pierre Lasjaunias Memorial Lecturer at the meeting of the World Federation of Interventional & Therapeutic Neuroradiology.
He is currently an Emeritus Professor at the University of York and is also one of the founders of Innovision-Ip Ltd where he is the Chief Scientific Officer

References

[1] BC Albensi, SM Knoblach, BGM Chew, MP O'Reilly, AI Faden, and JJ Pekar. Diffusion and high resolution mri of traumatic brain injury in rats: Time course and correlation with histology. *EXPERIMENTAL NEUROLOGY*, 162(1):61–72, MAR 2000.

[2] PJ Basser, J Mattiello, and D Lebihan. Estimation of the effective self-diffusion tensor from the nmr spin-echo. *JOURNAL OF MAGNETIC RESONANCE SERIES B*, 103(3):247–254, MAR 1994.

[3] Susan Y. Bookheimer, David H. Salat, Melissa Terpstra, Beau M. Ances, Deanna M. Barch, Randy L. Buckner, Gregory C. Burgess, Sandra W. Curtiss, Mirella Diaz-Santos, Jennifer Stine Elam, Bruce Fischl, Douglas N. Greve, Hannah A. Hagy, Michael P. Harms, Olivia M. Hatch, Trey Hedden, Cynthia Hodge, Kevin C. Japardi, Taylor P. Kuhn, Timothy K. Ly, Stephen M. Smith, Leah H. Somerville, Kamil Ugurbil, Andre van der Kouwe, David Van Essen, Roger P. Woods, and Essa Yacoub. The lifespan human connectome project in aging: An overview. *NEUROIMAGE*, 185:335–348, JAN 15 2019.

[4] Matthew D. Budde, Joong Hee Kim, Hsiao-Fang Liang, Robert E. Schmidt, John H. Russell, Anne H. Cross, and Sheng-Kwei Song. Toward accurate diagnosis of white matter pathology using diffusion tensor imaging. *MAGNETIC RESONANCE IN MEDICINE*, 57(4):688–695, APR 2007.

[5] Jennifer Stine Elam, Matthew F. Glasser, Michael P. Harms, Stamatios N. Sotiropoulos, Jesper L. R. Andersson, Gregory C. Burgess, Sandra W. Curtiss, Robert Oostenveld, Linda J. Larson-Prior, Jan-Mathijs Schoffelen, Michael R. Hodge, Eileen A. Cler, Daniel M. Marcus, Deanna M. Barch, Essa Yacoub, Stephen M. Smith, Kamil Ugurbil, and David C. Van Essen. The human connectome project: A retrospective. *NEUROIMAGE*, 244, DEC 1 2021.

[6] Chase R. Figley, Md Nasir Uddin, Kaihim Wong, Jennifer Kornelsen, Josep Puig, and Teresa D. Figley. Potential pitfalls of using fractional anisotropy, axial diffusivity, and radial diffusivity as biomarkers of cerebral white matter microstructure. *FRONTIERS IN NEUROSCIENCE*, 15, JAN 14 2022.

[7] David B. FitzGerald and Bruce A. Crosson. Diffusion weighted imaging and neuropsychological correlates in adults with mild traumatic brain injury. *INTERNATIONAL JOURNAL OF PSYCHOPHYSIOLOGY*, 82(1, SI):79–85, OCT 2011.

[8] Anne M. Hudak, Lifang Peng, Carlos Marquez de la Plata, John Thottakara, Carol Moore, Caryn Harper, Roderick McColl, Evelyn Babcock, and Ramon Diaz-Arrastia. Cytotoxic and vasogenic cerebral oedema in traumatic brain injury: Assessment with flair and dwi imaging. *BRAIN INJURY*, 28(12):1602–1609, 2014.

[9] Elizabeth B. Hutchinson, Susan C. Schwerin, Alexandru V. Avram, Sharon L. Juliano, and Carlo Pierpaoli. Diffusion mri and the detection of alterations following traumatic brain injury. *JOURNAL OF NEUROSCIENCE RESEARCH*, 96(4, SI):612–625, APR 2018.

[10] M Inglese, S Makani, G Johnson, BA Cohen, JA Silver, O Gonen, and RI Grossman. Diffuse axonal injury in mild traumatic brain injury: a diffusion tensor imaging study. *JOURNAL OF NEUROSURGERY*, 103(2):298–303, AUG 2005.

[11] Eunkyung Kim, Roh-Eul Yoo, Min Yong Seong, and Byung-Mo Oh. A systematic review and data synthesis of longitudinal changes in white matter integrity after mild traumatic brain injury assessed by diffusion tensor imaging in adults. *EUROPEAN JOURNAL OF RADIOLOGY*, 147, FEB 2022.

[12] Hannah M. Lindsey, Cooper B. Hodges, Kaitlyn M. Greer, Elisabeth A. Wilde, and Tricia L. Merkley. Diffusion-weighted imaging in mild traumatic brain injury: A systematic review of the literature. *NEUROPSYCHOLOGY REVIEW*.

[13] Yin Liu, Liyan Lu, Fengfang Li, and Yu-Chen Chen. Neuropathological mechanisms of mild traumatic brain injury: A perspective from multimodal magnetic resonance imaging. *FRONTIERS IN NEUROSCIENCE*, 16, JUN 17 2022.

[14] Ding Lyu, Runzhou Zhou, Chin-hsu Lin, Priya Prasad, and Liying Zhang. Development and validation of a new anisotropic visco-hyperelastic human head finite element model capable of predicting multiple brain injuries. *FRONTIERS IN BIOENGINEERING AND BIOTECHNOLOGY*, 10, MAR 24 2022.

[15] TE Nichols and AP Holmes. Nonparametric permutation tests for functional neuroimaging: A primer with examples. *HUMAN BRAIN MAPPING*, 15(1):1–25, JAN 2002.

[16] A Schwartzman, RF Dougherty, and JE Taylor. Cross-subject comparison of principal diffusion direction maps. *MAGNETIC RESONANCE IN MEDICINE*, 53(6):1423–1431, JUN 2005.

[17] Stephen M. Smith, Mark Jenkinson, Heidi Johansen-Berg, Daniel Rueckert, Thomas E. Nichols, Clare E. Mackay, Kate E. Watkins, Olga Ciccarelli, M. Zaheer Cader, Paul M. Matthews, and Timothy E. J. Behrens. Tract-based spatial statistics: Voxelwise analysis of multi-subject diffusion data. *NEUROIMAGE*, 31(4):1487–1505, JUL 15 2006.

[18] SK Song, J Yoshino, TQ Le, SJ Lin, SW Sun, AH Cross, and RC Armstrong. Demyelination increases radial diffusivity in corpus callosum of mouse brain. *NEUROIMAGE*, 26(1):132–140, MAY 15 2005.

[19] Tsang-Wei Tu, Rashida A. Williams, Jacob D. Lescher, Neekita Jikaria, L. Christine Turtzo, and Joseph A. Frank. Radiological-pathological correlation of diffusion tensor and magnetization transfer imaging in a closed head traumatic brain injury model. *ANNALS OF NEUROLOGY*, 79(6):907–920, JUN 2016.

[20] HP Van Putten, MG Bouwhuis, JP Muizelaar, BG Lyeth, and RF Berman. Diffusion-weighted imaging of edema following traumatic brain injury in rats: Effects of secondary hypoxia. *JOURNAL OF NEUROTRAUMA*, 22(8):857–872, AUG 2005.

[21] Jie Yang, Qian Li, Zhongyu Wang, Cunfang Qi, Xiaoning Han, Xi Lan, Jieru Wan, Wenzhu Wang, Xiaochun Zhao, Zhipeng Hou, Cong Gao, J. Ricardo Carhuapoma, Susumu Mori, Jiangyang Zhang, and Jian Wang. Multimodality mri assessment of grey and white matter injury and blood-brain barrier disruption after intracerebral haemorrhage in mice. *SCIENTIFIC REPORTS*, 7, JAN 13 2017.

[22] Fang-Cheng Yeh, Andrei Irimia, Dhiego Chaves de Almeida Bastos, and Alexandra J. Golby. Tractography methods and findings in brain tumors and traumatic brain injury. *NEUROIMAGE*, 245, DEC 15 2021.